D8.13 Lessons learnt to draw business models in use case SE#5
Version 1.0

Deliverable D8.13

30/06/2019

This project has received funding
from the European Union's Horizon 2020
research and innovation programme under
grant agreement n°731289

ID & Title:	D8.13 Lessons learnt to draw business models in use case SE#5		
Version:	V1.0	Number of pages:	46

Short Description

D8.13 Lessons learnt to draw business models in use case #5

Revision history

Version	Date	Modifications' nature	Author
V0.1	10-02-2019	Report structure	Pauline Ahlgren
V0.2	20-05-2019	Development approach and simulation results	Hendrik Flamme Gonca Gürses-Tran
V0.3	28-05-2019	Implementation approach and results	Pauline Ahlgren Fabian Regier
V0.4	10-06-2019	Peer-Review	Stanislav Hes
V0.5	11-06-2019	Additional Input	Demijan Panic
v0.7	25-06-2019	Final review from RWTH	Hendrik Flamme
V1.0	27-06-2019	Final review from E.ON	Fabian Regier, Jörgen Rosvall

Accessibility

☒Public	☐ Consortium + EC	☐ Restricted to a specific group + EC	☐ Confidential + EC

Owner/Main responsible

Name(s)	Function	Company	Visa
Peder Kjellén	WP8 Demo leader	E.ON	

Author(s)/contributor(s): company name(s)

Fabian Regier, Pauline Ahlgren, Michael Hirst, Hendrik Flamme, Gonca Gürses-Tran, Marco Cupelli, Jörgen Rosvall

Reviewer(s): company name(s)

Company	Name(s)
CEZ Distribuce	Stanislav Hes

Approver(s): company name(s)

Company	Name(s)
Enedis	Christian Dumbs

Work Package ID	WP8	Task ID	T8.11

Disclaimer: This report reflects only the author's view and the Agency is not responsible for any use that may be made of the information it contains.

EXECUTIVE SUMMARY

The transition to a low-carbon energy system requires a high penetration of renewable energy sources (RES) and efficient utilization of energy. The incorporation of intermittent RES entails challenges due to variable power output, stressing the need for flexibility options able to provide a balanced grid. Within the framework of the EU-funded INTERFLEX, a demonstration project has been implemented by E.ON to integrate and test innovative flexibility solutions in smart grids. The demonstration, located in the village of Simris in southern Sweden, encompasses operating a local microgrid (MG) with islanding capability and the ability to power the system by using only renewable energy sources. The overall objective is to demonstrate that a distribution system operator (DSO) can actively observe and smartly use the rural MG's ability to respond to merit orders for flexibility.

To meet this objective, the demonstration encompasses three use cases, in particular use case 3, 4 and 5 in Interflex terminology. The aim of use case 5, the focus of this deliverable, is to increase the ability to observe and steer the operations of a MG in response to distribution network constraints and enhanced control of the MG based on the use of advanced power analytics. The use case was evaluated in collaboration between RWTH Aachen University and E.ON Energidistribution AB. Theoretical simulations and development of advanced power analytics have been conducted by RWTH Aachen University to enable an in-depth evaluation of the developed forecasting and control strategies. In parallel, E.ON has developed forecasting and optimized control methods adapted to the conditions in Simris. E.ON further assessed the use case from a techno-economic perspective.

Development of advanced control strategies as well as data analytics algorithms was conducted to investigate how to leverage the increased ability to observe and steer a microgrid based on the distribution network requirements and constraints. This included the deployment of an electrical grid model of the Simris trial site to simulate grid behaviour. Two forecasting techniques were evaluated: while both techniques are using a sequence-to-sequence learning approach, one is based on recurrent neural networks (RNN) and the other one is based on convolutional RNN which aims at exploiting spatio-temporal dependencies. To optimize the system operation, a model predictive control (MPC) approach is used. Based on the simulation of the grid model, the controller optimizes its control input at each time-step in a receding horizon fashion. One major advantage is that the approach facilitates to easily incorporate forecasting methods. Moreover, the implementation allows to optimize various different objectives, such as potential islanding time maximization or loss minimization.
Furthermore, a multi-MG scenario, where each MG as well as the DSO are viewed as agents, was investigated. In this scenario, each agent aims at optimizing its individual objective within an agent-based concept. A bargaining algorithm is used to find a reasonable allocation of resources. The concept can be easily adapted to other scenarios.

Two optimal forecasting approaches were tested. Firstly, wind generation data, solar generation data and consumption data were separately used to train machine learning (ML) models. The second approach uses all of the three forecasted quantities to train one single ML model. The solutions were evaluated from a techno-economic perspective, comparing a rule-based control system with a control system comprising an intelligence module with forecast and optimization algorithms. The result showed that more than 10 % can be saved when incorporating an intelligence module.

The usage of model predictive control or optimization methods in conjunction with forecasting is from a technical as well as an economic perspective beneficial. Forecasts may

achieve a better accuracy if a higher quantity of measuring points and an installation of measurement points in different heights is applied. Implementation of model predictive control or agent-based control on the project site are worth investigation as next steps.

TABLE OF CONTENT

LIST OF FIGURES

LIST OF TABLES

1 INTRODUCTION

1.1 Scope of the document

The aim of this deliverable report is to describe:

- Steering of the Microgrid under 100% renewable generation while islanded
  - Rule-based control
  - Model Predictive Control
- Development of forecasting and optimization methods
- Assessment of the techno-economic impact of forecasting and optimization algorithms

1.2 Notations, abbreviations and acronyms

The table below provides an overview of the notations, abbreviations and acronyms used in this report.

Table 1: List of notations, abbreviations and accronyms

BESS	Battery Electrical Storage System
CNN	Convolutional Neural Network
COP	Heat-to-power-factor
DER	Distributed Energy Resources
DN	Distribution Network
DSO	Distribution System Operator
DSR	Demand Side Response
EMS	Energy Management System
HWB	Hot Water Boiler
LES	Local Energy System
LSTM	Long Short-Term Memory
MG	Microgrid
ML	Machine Learning
MPC	Model Predictive Control
NN	Neural Network
PCC	Point of Common Coupling
PIT	Potential Islanding Time
PQ load	Active and reactive load
PV	Photovoltaics
RBC	Rule-based control
RES	Renewable Energy Sources
RF	Random Forest
RNN	Recurrent neural network
SoC	State of Charge
SVM	Support vector machine
WTG	Wind Turbine Generator
R^2	Coefficient of determination (R-squared) indicates the proportionate amount of variation
RMSE	Root-mean-square error

2 DESCRIPTION OF USE CASE

The demonstration, implemented in Simris in Southern Sweden, encompass operating a local microgrid with the capability of 100 % island mode and being powered by 100 % of renewable sources. The overall objective is to demonstrate that a DSO can actively observe and smartly use the rural micro-grid's ability to respond to merit orders for flexibility. To meet this objective, the demonstration encompasses three use cases. The aim of use case 5 and focus for this deliverable, is to increase the ability to observe and steer the operations of a micro-grid in response to distribution network constraints and enhanced control of the micro-grid based on the use of advanced power analytics.

Detailed description of the local energy system at Simris

In 2015 E.ON Energidistribution decided to start the design and development of a pilot trial. This trial would be able to demonstrate that an electrical system can host a penetration of up to 100% power sourced from renewable sources (PV and Wind) by using field-proven, currently market available technologies. This trial would also prove that as a company it possesses the technical capabilities to deliver such a system.

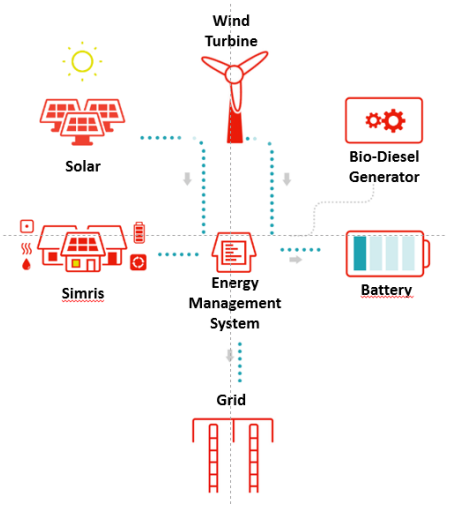

Figure 1: Overview of Simris project site

The small village of Simris in the south of Sweden was selected as pilot due to their optimal technical conditions including a pre-existing PV farm and wind turbine connected to their electricity grid (see Figure 1). A Battery Electrical Storage System (BESS) and a bio-fuel backup generator are also included (see Table 2). Along with a central microgrid controller, the system has the capability to seamlessly switch between interconnected and islanded mode.

Table 2: Parts of the Simris project

Production/Storage Asset; Project Site	**Power**	**Production / Storage / Consumption**
Wind Turbine	500 kW	1.4 GWh/a
Solar	440 kWp	0.45 GWh/a
Battery	833 kW	333 kWh
HVO	480 kW	*Island mode dependent*
Simris	Variable	2.1 GWh

3 APPROACH

The use case was evaluated by E.ON in collaboration with RWTH Aachen University. Theoretical simulations and development of advanced power analytics has been conducted by RWTH Aachen University and allow an in-depth evaluation of selected forecasting and optimized control strategies (see Section 3.1 and Section 4). In parallel, E.ON has developed forecasting and optimized control adapted to the conditions of Simris (see Section 3.2 and 5) and also assessed the use case 5 from a techno-economic perspective (see Section 3.3 and 6).

3.1 Development of power analytics algorithms

To investigate how to leverage the increased ability to observe and steer a microgrid based on the distribution network requirements and constraints, advanced control strategies and data analytic algorithms were developed.

The focus lies on utility microgrids (MGs) that are connected to the utility grid by a point of common coupling (PCC). They present an assemble of DER, incorporating residential or commercial loads, small scale controllable and volatile generation, energy storage systems and include auxiliary services such as DSR.

A general, hierarchical control structure has been developed, that separates control tasks into different levels and time horizons. Concepts are derived from the hierarchical control in transmission grids, compare [1], and adjusted for the needs of Distribution Networks (DNs) and MGs in particular [2, 3, 4, 5].

In order to evaluate different control strategies, it is necessary to accurately model the microgrid. Section 3.1.1 describes the grid model that has been developed to realistically simulate the Simris test site. The forecasting approaches developed within this project are discussed in section 3.1.2. Section 3.1.3 describes an advanced control strategy – in particular Model Predictive Control (MPC) – which is a natural candidate to facilitate the incorporation of forecasts in a control scheme. Based on the developed centralized MPC algorithm, an agent-based concept is derived to investigate the impact of conflicting interests of different agents on the DSO. Subsequently, section 3.1.5 provides a brief summary of this chapter.

3.1.1 Electrical Grid Model

In order to simulate grid behavior, a realistic model of the Simris test site was developed. To facilitate simulating a wide range of different scenarios, a quasi-continuous model design was chosen to allow to accurately describe the essential dynamic characteristics of the system. The simulation is implemented in MATLAB Simulink. The grid model and the energy management system (EMS) control are tied closely together. This section will describe the model including the problem setup. Section 3.1.2 describes the forecasting methods, while section 3.1.3 focuses on the MPC algorithm itself. A thorough elaboration on the grid model can be found in our InterFlex publications [6], [7] and [8].

The three-phase representation of the grid model consists of different components: residential loads, batteries, heat pumps, hot water boilers, photovoltaics, wind turbines,

micro turbines as well as network components such as lines, transformers and a circuit breaker (see appendix 10.2). Each component is represented as a Simulink block with variable block parameters. The whole set of block definitions is established in a customized microgrid library. Furthermore, the developed model allows to add additional component types such as fuel cells and electric vehicle charging stations.

3.1.2 Forecast Algorithms

In the context of power systems, forecasts can essentially be classified according to their time horizon. Long-term power system planning requires predicting and interpreting trends such as additional loads, urbanization and changing energy policies.
Short-term forecasts on the other hand are used to operate the power system in a reliable and efficient manner. This work investigates the application of short-term forecasting algorithms to facilitate efficient scheduling of flexibilities in a microgrid. The goal is to develop forecasting approaches that could be deployed on the test site in Simris.

The energy management system of a microgrid has to deal with a large amount of uncertainty due to the volatility of renewables – in particular solar and wind – and the fluctuating energy consumption of individual households. While power consumption - aggregated on utility level - shows low variability, it is highly intermittent with low periodicity on a microgrid scale. Renewables show similar, less distinct aggregation effects. Providing accurate forecasts of both consumption and generation is vital for an efficient dispatch of available flexibilities in order to prolong potential islanding time, reduce costs or reduce carbon dioxide emissions.

An artificial neural network (ANN or NN) is a highly flexible computational model that is inspired by the human nervous system. The so-called neurons are structured in layers so that an input vector is mapped to an output vector (see Figure 19). Figure 2 depicts a simple (feed-forward) neural network with multiple layers. However, recurrent neural networks (RNNs) have layers that are also connected to some preceding layer, thus creating a loop. RNNs are particularly useful for time-series forecasting problems as these cyclic connections are well-suited to capture the dynamic behavior of the sequence. There are some well-established structures that implement cyclic connections. The most popular one is the *long short-term memory* (LSTM) cell [9], which is illustrated in Figure 20. In particular, the LN-LSTM cell, which adds *layer normalization* [10] in between each hidden layer, is used.

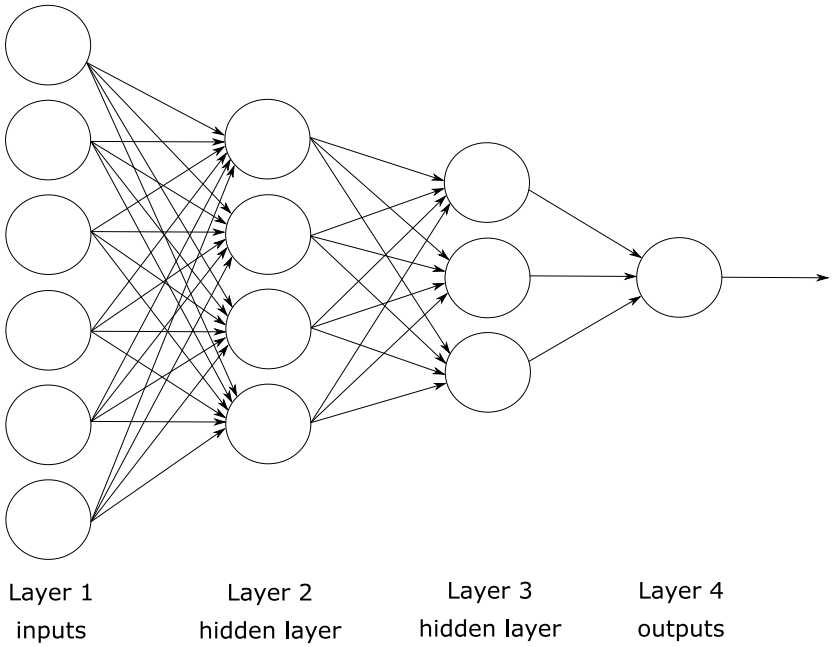

Figure 2: Depiction of a layer-wise architecture of a simple feed-forward neural network. Each circle represents a neuron.

Sequence-to-sequence learning

In the course of the project, a sequence-to-sequence RNN forecasting architecture had been developed. Figure 3 illustrates the basic structure when the network is rolled out over time. The neural network consists of two separate sub-networks: the encoder and the decoder. The encoder works in a receding horizon fashion. When all data samples until the current point in time have been fed into the network, the hidden state is passed on to the decoder. The idea is that the encoder embeds the relevant characteristics of the historic sequence into a vector, the hidden state. The decoder, on the other hand, uses this hidden state to generate forecasts of the quantity of interest (see in Figure 3). Please see [11] for detail.

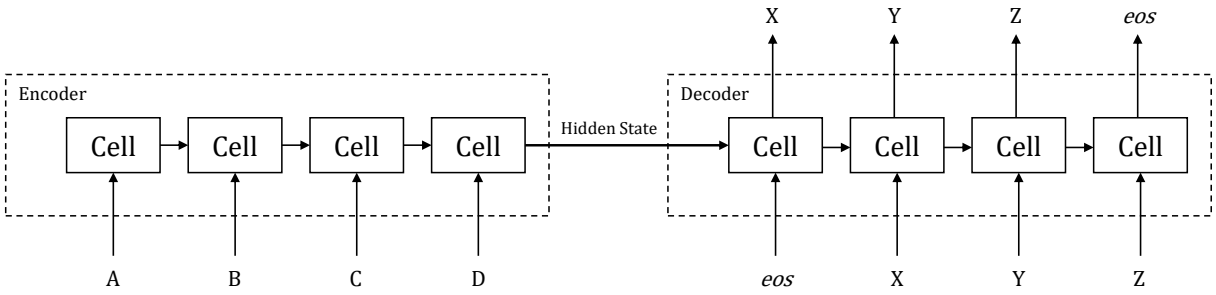

Figure 3: Sequence-to-sequence architecture from [11].

The proposed forecasting architecture aims at exploiting auto-regressive as well as supplementary, exogenous variables. To do so, the architecture must be trained using historic data. The training process is an iterative process:

1. As a first step, the inputs are fed into and passed through the network, which is called *forward pass*.
2. A *loss function* evaluates the accuracy of the fit between the model's prediction and the associated target value.
3. In the *backward pass*, the partial derivatives of the loss function with respect to all trainable network parameters are calculated using backpropagation. [12]

4. In the stochastic gradient descent step, the network parameters are updated based on the *learning rate* and the previously computed gradient. The learning rate defines the amount by which the weights are updated along the gradient.

The *hyperparameters* are the model parameters specifying architectural and training process properties that cannot be learned such as the number of hidden layers, the number of units per layer or the learning rate. However, the outcome of the training process is highly sensitive about the hyperparameters. *Random search* trains several different versions of the architecture with randomly chosen hyperparameters to find a suitable set. It is generally superior to *grid search* [13], where the hyperparameter space is evaluated at equidistant points.

A strong performance on the training data is not a valid way to assess the model's performance as we want the model to generalize to new data. The developed model uses *dropout* [14] as *regularization* technique to reduce the effect of overfitting. For each sample, dropout ignores a randomly chosen set of neurons. That way the network is forced to focus its learning attempts on the essential patterns. It can be interpreted as training an ensemble of neural networks [15].

The sequence-to-sequence forecasting approach is applicable to many different scenarios such as solar, load and wind forecasting. However, performing very short-term wind forecasts remains challenging in practice due to the high stochasticity. Figure 17 shows that wind time-series tend to have a short auto-correlation. To improve wind forecasts, a new architecture is developed that includes wind speed and wind direction from neighboring measurement devices. The idea is that the information of distributed, scattered measurement devices may improve the forecast by exploiting spatio-temporal dependencies. The following forecasting approach is entirely based on our Interflex publication [16]. The goal of this section, however, is to present the concept of the approach.

Convolutional LSTM architecture

Convolutional neural networks (CNN) are widely used in image recognition. Their strength is to capture patterns in data with spatial dependencies such as images. Essentially, convolutional neural networks differ from fully-connected neurons in that they only have connections to neurons that represent adjacent input cells, constituting a receptive field. A convolutional layer has several hyperparameters such as the *kernel size*, which defines the size of the receptive field. If stacked together, different levels of abstraction can be achieved.

Within this work, CNNs are combined with RNNs to combine CNN's spatial with RNN's temporal mapping capabilities. Analogously to pixels in image recognition, wind forecasts from different weather stations or wind farms will provide the spatial dimension, while the individual time-series data constitute the temporal dimension. Convolutional LSTM (convLSTM) cells [17] combine the concepts of CNN and RNN. They take a 4D input tensor, where two dimensions represent the spatial dimension, one dimension is reserved for the time dimension and the remaining dimension is used to accommodate more than one input variable per time-step and spatial location.

The model size, e.g. the number of layer-wise feature maps, as well as other hyperparameters are tuned using random search. The preparation and reshaping of the data is discusses in section 4.2.2. For more details on this approach, refer to [16].

3.1.3 Control Strategies

The developed simulation models incorporate the RBC as a reference control scheme, which serves as a benchmark to evaluate the performance and adequacy of the developed advanced control scheme, further explained later.
All variants of the control methods have been tested in simulation first on open source test grid data and later for the SIMRIS trial site. A schematic representation of the site under study with the main parameters is presented in Figure 4.

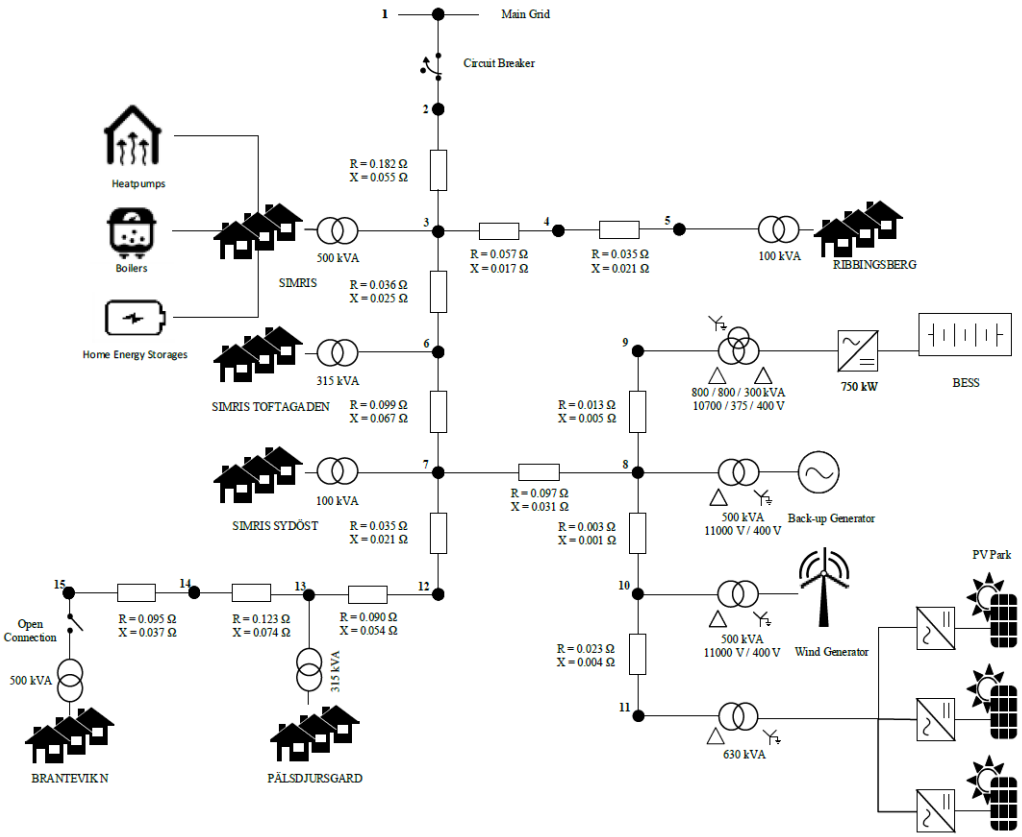

Figure 4: Schematic representation of the MG test site [18]

Reference Control Scheme

The basic control of the flexibilities, e.g. batteries, heat pumps etc., is realized using the RBC. The RBC is a simple expert-based heuristic, that has been developed by the DSO in an empirical step-by-step approach. For instance, if the SOC of the large microgrid battery surpasses a certain threshold, the DSR assets are activated or deactivated to provide flexibility. It had also been implemented in simulation as a reference for the Model Predictive Control (MPC) that will subsequently be discussed. Results of a first representation and elaboration on the RBC, in comparison to the developed MPC, have been published and presented earlier [18].

In a next step, the RBC has been optimized especially with regard to the functionalities of the thermally coupled elements, i.e. heat pumps and hot tap water boilers. It is important to note that they only allow to be controlled in such a way that the electric load increases. An upward control allows to override the original heating profile and heat at maximum power until a threshold is reached. The downward control is limited due to negative influence on the customers' comfort.

An accurate representation of each thermal device of the test site would have exceeded the use case's scope. By factoring in generic building characteristics, heat demand and real temperature data, the proposed approximation of the control characteristics is of great value for the determination of the flexibility potential. The heat controller attempts to reduce the gap between the current and the target temperature. In the end, the thermal power of the heat controllers is measured and converted to electric power using the COP ratio so that the resulting power can be applied to the dynamic load.

Model Predictive Control

In contrast to classical control methods that do not require a system model, model predictive control (MPC) solves the control task by optimizing the simulated behavior of the system over a receding horizon. Figure 5 illustrates the MPC concept. The red line represents the output *y* of the controlled system while the blue curve represents the control input *u*. In other words, at each time step, MPC solves an optimization problem to retrieve the optimal control inputs over the entire horizon. The first control input $u(t)$ is then applied to the system while the remaining control inputs are discarded. This procedure is repeated at every time step, which - contrary to traditional optimal control - induces a feedback loop. Performing an optimization over a certain horizon requires to accurately simulate the power system over that horizon.

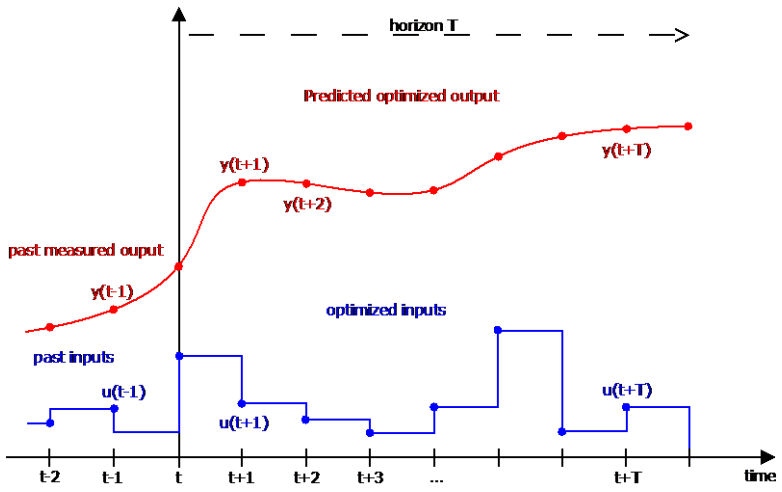

Figure 5: Illustration of the model predictive control concept

In the Simulink development, in order to enable the MPC simulation, the forecast errors on future grid states can either be selected to be zero, to follow a uniform or Gaussian distribution (see Figure 6). In this case, the files which include the predicted values for future demand and generation profiles at each bus are generated automatically and stored in the MATLAB workspace. The forecasting algorithms that have been developed and

described in section 3.1.2, can be integrated in the MPC. For this, the results are imported from external as csv files.

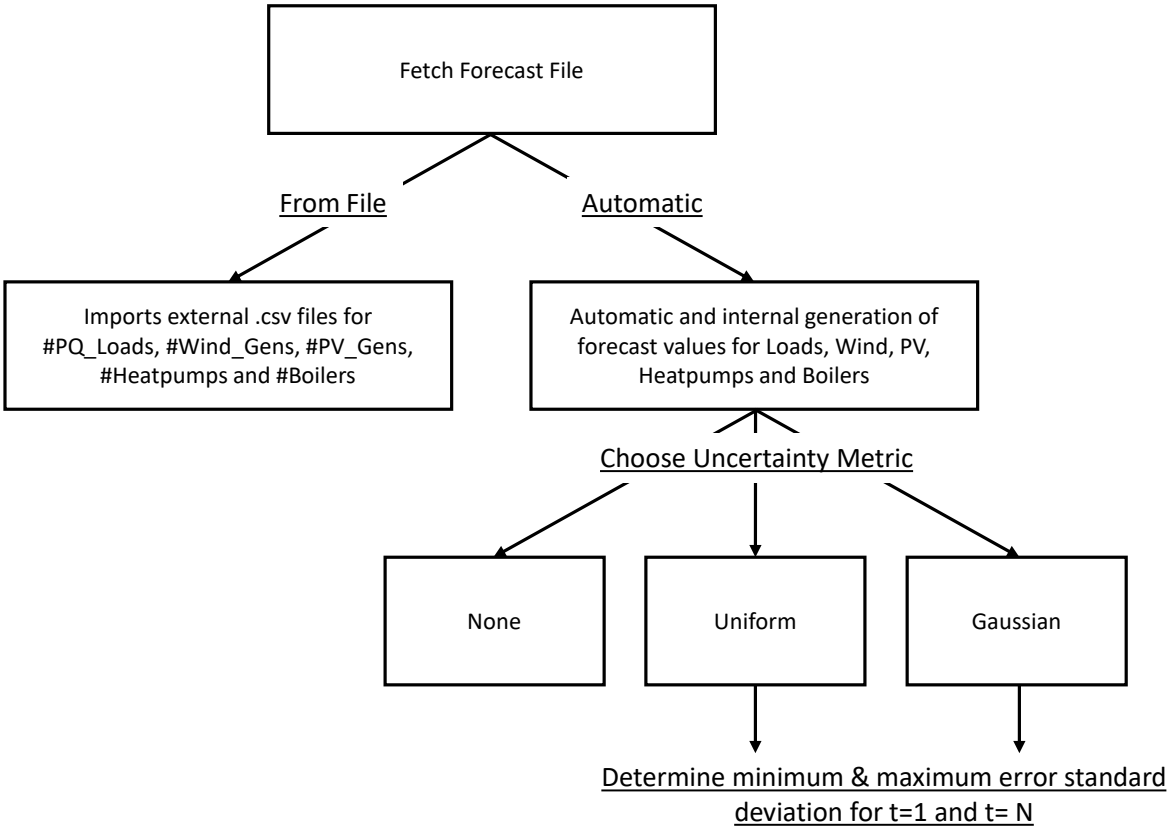

Figure 6: Loading forecasts into the MPC model

The grid model that had been developed in section 3.1.1 is used to simulate the system. Formulating the control task as an optimization problem allows to take forecasting methods - such as those developed in section 3.1.2 – into account. Moreover, the constraints of the different components are taken into account. Earlier publications reveal the developed constraint representation [6], whereas classical control leaves those out of consideration. The developed MPC allows multiple objective functions such as loss minimization, power exchange minimization and algorithmically more complex objectives, such as potential islanding time maximization. We will further elaborate on those in section 4.3.

3.1.4 Agent-based Concept

In order to investigate the impact of an agent-based concept on the DSO, a multi-microgrid scenario is considered, where each microgrid EMS represents an agent. Based on the Simris test site, a distribution network model was created that incorporates multiple microgrids. Figure 21 depicts the network and also illustrated the composition of the MGs. Each microgrid can act autonomously within its network boundaries and thus pursue individual objectives. The objective functions may be chosen arbitrarily as long as they map to cost, e.g. an MG may choose to maximize potential islanding time by encoding it using a value/cost function. This way each agent minimizes a cost function, which allows comparability and trading with each other. The DSO steers the network that connects the microgrids with one another as well as with the main grid. To verify the concept, a simplified DN is assumed.

The DSO constitutes another agent with its own objectives. Again, these objectives can be arbitrary assuming that they represent costs, such as reducing power losses, performing peak shaving or avoiding other penalties. The idea is to study the case where the microgrids can choose their schedule (through optimization) independently of the DSO's needs. They may trade power with each other or with the wholesale market, which is accessible via the main grid connection.

In a first step, the set of microgrids is optimized without considering the objectives and constraints of the DSO. Based on the resulting power schedules, which are optimal for the microgrids, a simple power flow in the distribution grid is carried out in order to evaluate the DSO's objective. The microgrid schedules and the associated costs as well as the DSO's cost serve as base case and will subsequently be refered to as *locally optimal schedules* and *cost*, respectively.
In another step, the entire system is optimized including the DSO's objective. Consequently, the individual microgrid schedules may change, leading to reduced cost of the entire system while the costs of some microgrids may increase. We will refer to the resulting schedules as *globally optimal schedules*. This raises the question on how the agents should share the benefit in cost reduction among each other. It is clear from a system perspective that these new schedules are preferable. However, as they might come with increased costs for some agents, they must be financially compensated.

We chose an axiomatic approach – in particular *Nash Bargaining Solution* (NBS) [19] – to derive a 'fair' agreement to the bargaining problem. In contrast to other bargaining approach, which focus on modeling the bargaining process itself, NBS only considers potential agreements that satisfy some 'reasonable' axioms. These axioms as stated by Nash in [19] are:

1. **Individual rationality**: As explained earlier, individual rationality means that an agent is only willing to collaborate and to find an agreement if it does not suffer under the consequences.
2. **Pareto efficiency**: A solution to a bargaining problem is called Pareto efficient if there exists no other potential agreement that allows any agent to improve its utility without deteriorating the utility of any other agent.
3. **Symmetry**: Symmetry means that the solution must not discriminate between two indistinguishable agents.
4. **Invariance to equivalent payoff representations**: If the utility function of an agent is subject to an order-preserving linear transformation, then the utility of the new solution should equal the transformed utility of the old solution.
5. **Independence of irrelevant alternatives**: Restricting the set of potential agreements without excluding the original solution to the problem must not alter the solution.

These axioms ensure that there is a unique solution to the bargaining problem. In this scenario the agents bargain about the payments that the DSO has to make or receive, respectively. The unique solution is retrieved by maximizing (1), where the payoff of the DSO is constituted by its cost at the disagreement point and the costs of an agreement as well as the payments between the agents (see appendix 10.4). Analogously, the payoff of each individual microgrid is a function of its costs and payments. The objective function ensures that the axioms 2 to 5 are fulfilled and the constraints enforce individual rationality.
In the context of the multi-microgrid scenario, the solution specifies how financial compensations due to change in cost that some agents face. As the cost of the entire system

is expected to decrease, the bargaining process leads to a mutually beneficial agreement. For more details, please refer to the corresponding publication [20].

3.1.5 Summary

The development approach for the power analytics algorithms was described. The first part focused on the electrical grid model. In particular, the model assumptions as well as the representation of the different components were discussed. Besides grid components such as transformers and lines, the model considers the characteristics of various microgrid components such as heat pumps, hot tap water boilers and micro turbines.
Subsequently, two forecasting techniques were discussed: a sequence-to-sequence learning approach based on LSTM cells and a model that aims at exploiting spatio-temporal dependencies using convolutional LSTM cells. The sequence-to-sequence algorithms is intended to serve as a general-purpose forecasting approach, whereas the second approach requires the availability of scattered measurements to improve the performance.

Moreover, the developed control strategies were described. The RBC is a simple expert-based heuristic that had been empirically developed by the DSO. It serves as the baseline control method in the simulation model. However, the RBC is not very sophisticated as it cannot incorporate supplementary information such as forecasts. The MPC approach works in a receding horizon fashion. At each time-step, it optimizes its control based on the simulation of the grid model. This way it can take forecasts into account. Furthermore, the developed MPC allows multiple objectives such as loss minimization or potential islanding time maximization.

Finally, an agent-based concept was derived in a multi-microgrid scenario where each MG as well as the DSO were regarded as agents. The method uses Nash bargaining solution to find an allocation of resources – in our case the usage of the distribution network - that balances the agents' conflicting interests based on a set of axioms. The concept can be easily adapted to other scenarios.

3.2 Development and implementation of project tailored solution

The project site in Simris consists of different assets necessary for electrical production, storage and consumption (see section 2). Figure 7 depicts an overview of the Simris architecture with its physical electric and informational connections. The electric connections are illustrated with the blue lines in this figure. The red dashed lines represent the communication lines. As seen above, the EMS serves as the main controller in the microgrid control system. The EMS has access to relevant information, such as measurements from current and voltage transformers, indication of status from power breakers and disconnectors.

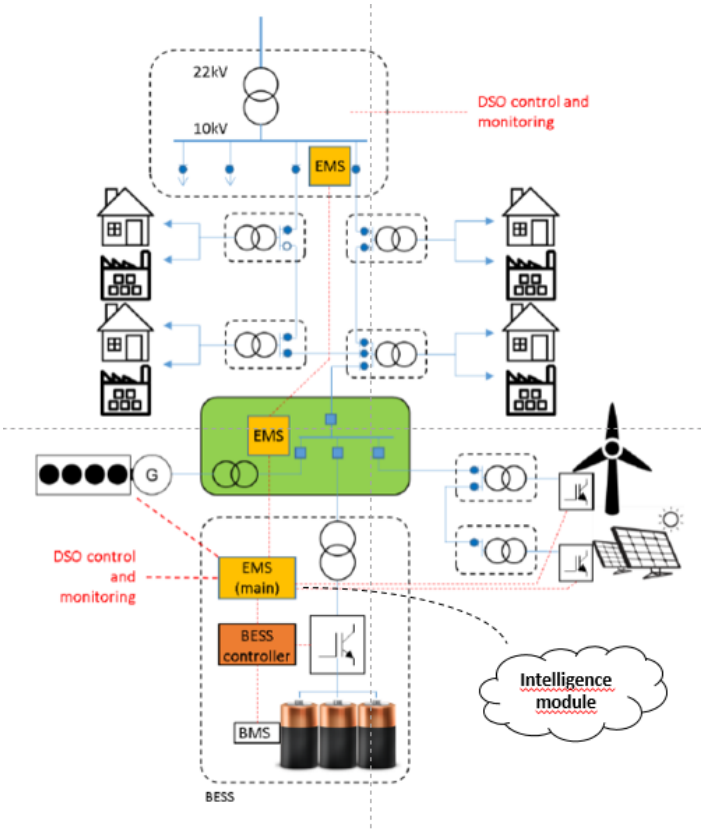

Figure 7: System and components of Simris

The physical arrangement at the Simris project site is demonstrated in Figure 8. The squares and circles show the power substations. The connections between them, in turquoise, present the actual powerlines. The network of the Local Energy System (LES) was created around an already existing grid. Within the grid, there are six secondary substations 11/0,4 kV with several customers connected. The number of connection points within the LES is 151. The feed in point to the LES is via a substation "SRS" 20/10 kV from a 10-kV bay (SRS bay 7). The bay is equipped with a power breaker, voltage and current transformers and relay protection devices. To the feeder at bay 7 (LES bay), there were existing PV and wind generation connected.

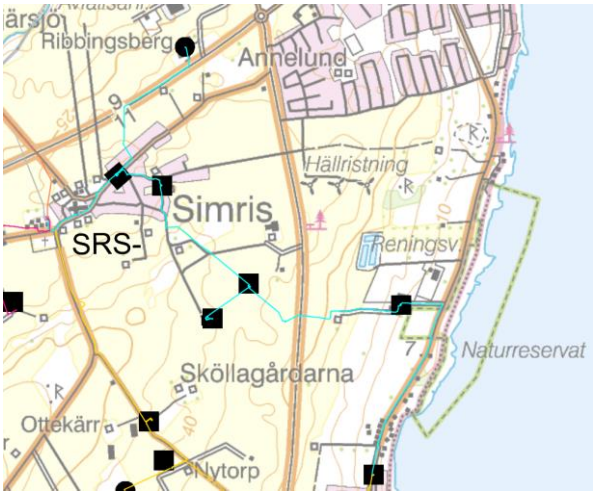

Figure 8: Screenshot of the Simris project site (GIS)

In the description of work, E.ON and RWTH Aachen has described how intelligent steering of the micro grid could help provide ancillary services to the main grid. The concept of this was taken one step further. We let the Simris village represent a single customer, a local energy community metered at a single point, from a conceptual point of view and developed an intelligence module designed to minimize the cost of energy for the customer. The intelligence consists of the following sub-modules:

1. Forecasting module able to forecast generation and demand in Simris,
2. Optimization module able to take the forecasted values as an input together with adjacent relevant information such as network tariff and produce an optimal set-point which is sent to the micro grids,
3. Energy Management System able to execute the optimal set-point given as an output front the optimization module as well as ensuring the integrity and safe operation of the micro grid.

The basic setting of the EMS is rule-based (See Section 3.2.3). The objective of this research is to compare the pure rule-based control method with advanced control algorithms for microgrid energy management. Therefore, an intelligence module consisting of a forecasting and an optimization tool was developed. The intelligence module has direct access to the EMS.

3.2.1 Forecast

The forecasting module is responsible for providing continuous consumption and generation forecast to the optimization module, which will utilize it to provide the asset steering strategy. The weather information based on wind-, solar- cloud cover and temperature prognosis. In some cases, the forecasts are combined with additional information such as the theoretical solar irradiation or information on the Swedish bank holidays, all playing a role in the different forecasting models.

The weather data feed-in for the forecasting module is imported data consisting of historical and forecast weather data from different providers. To improve accuracy a weather station near the village of Simris was chosen. Generation and consumption data are collected directly by the EMS. This means that as soon as data from a new customer is connected to the cloud, the forecasting module can read the new customer data and run.

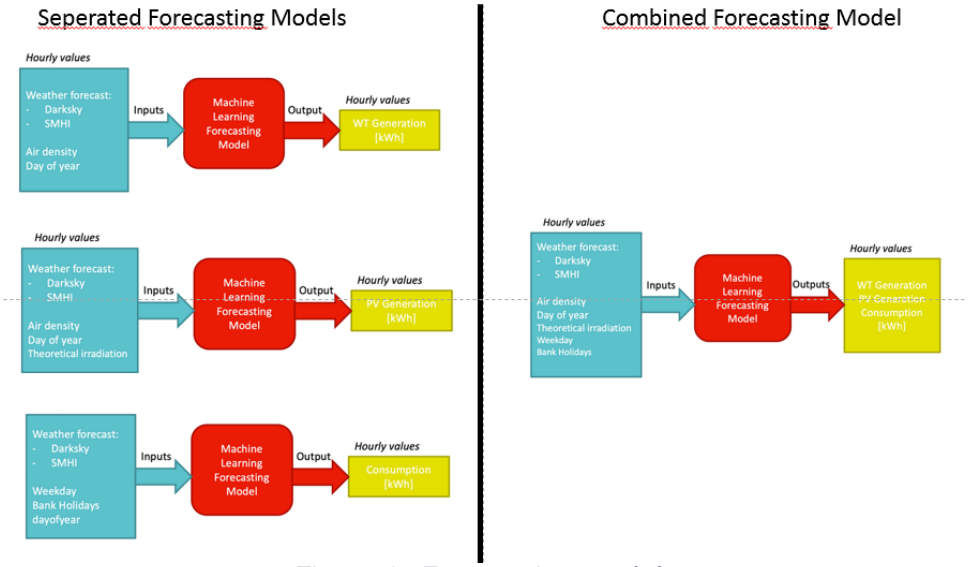

Figure 9: Forecasting models

Two approaches of the optimal forecasting method were tested. The first approach encompassed combining a single machine learning (ML) model with the exact data concerning wind generation, solar generation or the consumption of the customer (Figure 9). The second approach was to combine all of the three forecasted quantities with one single ML model.

Training is done with historical data based on hourly measurements and starting from September 2017. The training period taken, equals or is greater than one year from September 2017. Eighty percent of the data within this training period is used for training the model, the remaining twenty percent being kept for testing purposes.
Machine learning models are known to age with time and slowly decrease their performance. regular retraining is thus a good way to always have up-to-date high performance.

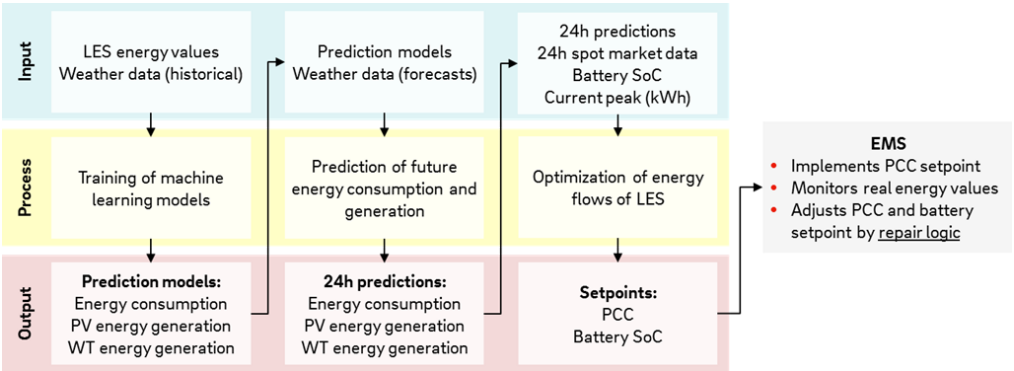

Figure 10: Intelligence module pipeline

Figure 10 shows the process of the intelligence module pipeline. The pipeline is iterative and runs regularly. It starts with training of the machine learning models with the input of LES energy values and historical weather data. As a result of the training prediction models for hourly consumption, PV generation and WT generation energy values are created. In the next step, future LES energy values are predicted using the trained prediction models and weather forecasts. This leads to an output of 24-hourly predictions of energy consumption, PV and WT Generation. That output is extended with 24 h spot market data, the SOC of the battery and the current peak (kWh) for further optimization.

3.2.2 Control method

The control mechanism follows fixed rules implemented in the energy management system and utilizes two stable differentiations. In the first state, the renewable energy production exceeds the load. The battery will be charged until it reaches the full capacity. If the generation is still higher than the consumption and the battery is full, further production will be sold to the grid. In the second state, the consumption level exceeds the production. In this case, the battery will discharge until it is empty. If the battery is empty, the energy deficit will be imported from the grid.

The optimization module calculates the optimal steering strategy for the LES based on predicted energy generation and consumption over the next 24 hours. The optimal steering strategy is based on the optimization objective specified. Based on the optimal steering strategy, steering signals are calculated and sent to the EMS. The EMS implements the steering signals and applies a repair logic, to account for deviations between the predicted energy values and actual energy values.

Optimization is based on a target function that aims to minimize or maximize on a defined optimization objective. Depending on the specific customer segment and market condition, different optimization objectives can be set. Possible optimization targets include total cost minimization, peak shaving and autarky maximization. Further optimization targets can be defined according to customer needs.

3.3 Economic consideration

To assess the impact of forecasting and optimization modules, a comparison of modules in terms of costs with different assumptions was conducted. Within a techno-economic model the costs are compared to different settings of technical input. To evaluate the benefits of forecasting or optimization modules, a baseline case without these capabilities is defined first. This baseline serves as a reference for the advanced control options. As such live data was conducted from the project site for a determined time span. With this fixed dataset different simulations have been conducted.
The first case shows the baseline. In the second case a perfect foresight for the whole period is considered. The third case describes a controller with a rolling optimization horizon. Hereby, the set-points for the upcoming 24 hours are optimized after each full hour. This approach therefore represents a limited forecast, that is updated on an hourly basis. Each case will provide a different output of costs. With comparing these costs, the impact of using optimization and forecasting tools can be evaluated.

Table 3: Cases for assessment of techno-economic impact

Case	Technical Setting	Foresight Level
1	Rule-based control	No foresight
2	EMS with optimization and forecasting module	Perfect foresight for the whole period

3	EMS with optimization and forecasting module	Perfect foresight for one day

As the outcome of the techno-economic model is based on simulations some constraints had to be defined. The two main constraints are that:

- the evaluated timespan considered not a full year but covers all seasonal variation,
- the costs are purely related to the market electricity pricing (e.g. no costs for the development considered).

Comparing the operational costs of the local energy system implemented in Simris with and without using forecasting or optimization modules gives us an idea of the impact of these modules. Section 6 shows the results of the different settings.

4 RESULTS OF THE POWER ANALYTICS SIMULATION

This chapter evaluates the methods that have been presented in chapter 3.1.

4.1 Electrical grid model

The grid model described in section 3.1.1 has been developed to primarily serve as a basis for the representation of the control schemes that are applied on the test site today and could be applied in future tests beyond the scope of the project.
The model allows to quantify bus voltages, phase, overcurrent and energy prices incurred, depending on the rule-based and optimized energy management and scheduling. The results, which are derived from the grid model are further elaborated in subsequent sections.

4.2 Forecast Algorithms

The following part describes the findings in [11] and [16] that had been discovered as part of the Interflex project. For more details, please refer to these publications.

The quality of the forecast and its accuracy depend strongly on the quality and quantity of the data. Within the short time span of this project, it was not possible to collect data to this extent and subsequently develop forecasting methods based on them. This is why the proposed sequence-to-sequence architecture is assessed using the Global Energy Forecasting Competition 2014 (GEFCom14) [21]. However, the developed forecasting methods are applicable to Simris and any future microgrid, given that the specified data requirements are met.

4.2.1 Sequence-to-sequence learning

Within this chapter we chose to elaborate on the load forecast, however, the proposed model can also deal with other quantities such as solar and wind. The GEFCom14 dataset contains hourly load measurements as target time-series and 25 auxiliary temperature readings including their time stamp. The total data set comprises 60,600 time steps. The first 80 % of the dataset are used for training, while the remaining data is used as test set to evaluate the model after the training process finished.
The data is normalized since neural networks genuinely perform better when all the inputs are within a similar range as the gradient descent update mechanism would otherwise be biased towards larger numerical values. Categorical features are one-hot encoded.

The hyperparameters of the neural network were tuned using *random search*. It was found that 2-4 hidden layers with 10-40 cells are sufficient to capture the main characteristics of the dataset. Increasing the complexity of the model will require an increase in the amount of normalization to prevent overfitting.

To assess the performance of the developed forecasting model, two state-of-the-art machine learning approaches were used. These were benchmarked against two classical time-series analysis (TSA) methods were used as benchmark. The machine learning methods comprise a standard RNN implemented following the best practice methodology description in [22], as well as a random forest regressor according to the description in [23]. Moreover, we apply

TSA-based forecasting using *second degree exponential smoothing* and *auto-regressive integrated moving average* (ARIMA). For exponential smoothing we employed the Python-based module pandas. The ARIMA model we implemented using the Python module statsmodels [24]. Three metrics were chosen to evaluate the developed model: The R^2 *accuracy measure*, the *root mean square error* (RMSE) and the *normalized RMSE* ($nRMSE_{\%}$) (see appendix 10.5).

Table 4 shows the test results for the different forecasting methods using the three metrics. The developed sequence-to-sequence architecture significantly outperforms the reference models on the GEFCom14 load dataset.

Table 4 : Results overview and comparison [11]

Method	R^2	RMSE	$nRMSE_{\%}$
Sequence-to-sequence RNN	*0.9497*	*10.82*	*3.59*
Standard RNN	*0.9168*	*14.37*	*4.77*
Random Forests	*0.8335*	*18.31*	*6.07*
ARIMA	*0.7553*	*18.72*	*6.21*
Exponential Smoothing	*0.6245*	*24.12*	*8.00*

The forecast horizon can be chosen arbitrarily and can be adjusted dynamically. However, the quality of the forecast degrades for a longer horizon as the inherent uncertainty increases and the outcome is based on previously forecasted values.
The developed method is applicable to other time-series forecasting problems as it is posed in a very generic form.

4.2.2 Convolutional LSTM architecture

The GEFCom14 dataset provides hourly readings of wind speed in $\vec{u}$ and $\vec{v}$ components for 10 different wind farms in Australia over a two-year horizon. The input data is reshaped to form a grid with a height of four and a width of five. The number of channels is two as the wind speed is measured both at 10m and 100m altitude. The data is restructured according to *Figure 11*. We denote the input shape as [4, 5, 2] and call the resulting architecture *convLSTM452*. Moreover, two architectures using input spaces of shape [5, 2, 4] and [2, 5, 4] have been trained.

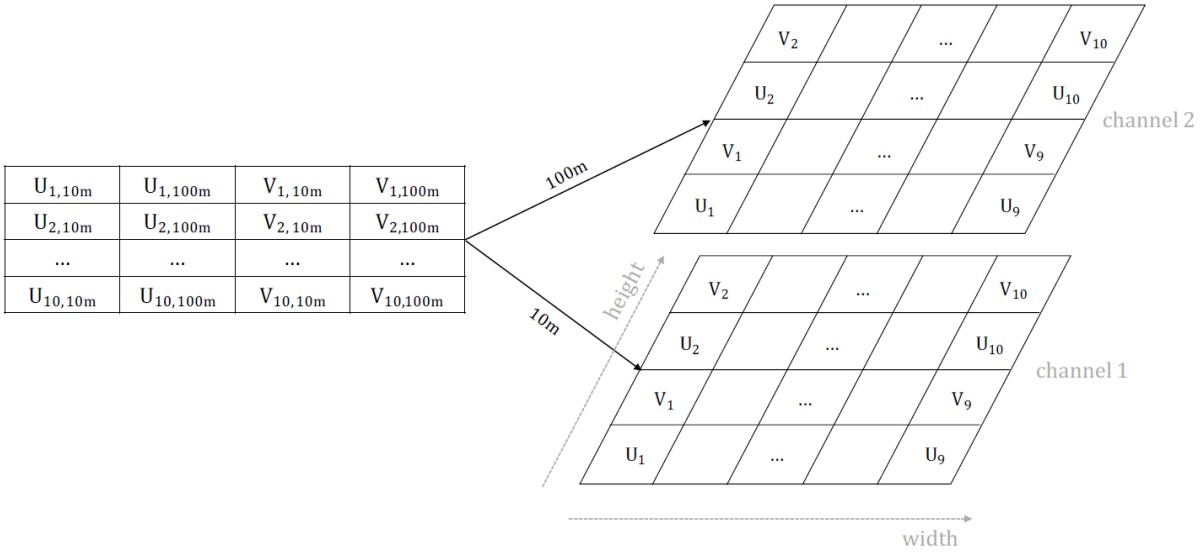

Figure 11: Feature reshaping of the GEFCom14 dataset into [4, 5, 2] shape [16]

Furthermore, a standard LSTM network, which follows the best practice implementation as described in [22], has been trained to assess the proposed approach. Moreover, a random forest regressor (RF) was implemented for comparison, following the best practice implementation in [23]. The RF was similarly trained by searching a reasonable hyperparameter space.

The proposed models as well as the reference models are evaluated using the same metrics. The evaluation results are shown in Table 5. convLSTM524 and convLSTM254 clearly outperform the standard LSTM model as well as the RF predictor. This suggests that the convLSTM cell is better suited to capture the spatio-temporal dependencies within wind power forecasts than the standard LSTM approach. The difference between convLSTM524 and convLSTM452 is suspected to be due to convLSTM524 resembling the actual relative geographical locations more closely. Therefore, we expect further improvements, i.e. improved accuracy of model with improved accuracy of weather data, if the input space matches the actual locations more accurately. For more details, refer to *[16].*

Table 5: Results overview and comparison [16]

Method	R^2	RMSE	$nRMSE_{\%}$
convLSTM452	*0.6696*	*0.1986*	*2.16*
convLSTM524	*0.7588*	*0.1697*	*1.84*
convLSTM254	*0.7688*	*0.1661*	*1.81*
Standard LSTM	*0.6115*	*0.2156*	*2.34*
Random Forests	*0.7216*	*0.1823*	*1.98*

4.3 Control Strategies

This section presents briefly the main results of the control study. The reference control scheme solely serves as a comparison to the developed advanced control and has been described in earlier publications [18]. With the advanced control mechanism only, an optimal dispatch of flexibilities is achieved. In addition, the MPC can easily be applied to more systems and can therefore serve for future scalability and flexibility analysis while the RBC is specifically parametrized for a certain grid configuration. Hence, the following subsections

comprise the MPC and the agent-based control, representing a central advanced control mechanism, and a distributed control optimization. In the last section, the agent-based concept is evaluated in a multi-MG scenario.

4.3.1 Model Predictive Control

In the earliest project studies, the developed MPC methodology has been tested on an open source test grid to allow a benchmark. The test system employed at that stage for investigating the effects of the proposed EMS is based on the Cigre LV MG benchmark [25, 26]. A residential system is considered, where private households are responsible for the bulk of the load. In addition, a variety of DER are regarded. The system is completed with input data series derived from physical and stochastic modeling, as well as with real world measurements. In a later stage, the optimized model has been applied on the Simris representation presented in section 3.1.1.

In [6], three different objective functions have been selected:

(a) cost minimization,
(b) power exchange minimization,
(c) autonomy maximization, which corresponds to potential islanding time (PIT) maximization.

The effect of these objectives and their direct influence on actually achievable PIT have been evaluated. It is shown that a trade-off always exists between the above-mentioned competing objectives. In particular, a minimization of concurrent power exchange with the main grid results in the reduction of reserves, which are then missing for a potential future islanding event.
Grid operation under each of the functional objectives (a)-(c) was first simulated over a horizon of three months in a generic microgrid with an MPC controller using one hour as controller sampling time with a given 24-hour prediction time horizon. In Figure 12 results are sorted by the hour of day in which the islanding event started. The resulting islanding time is grouped in 15-minute bins as relative shares of islanding occurrences.

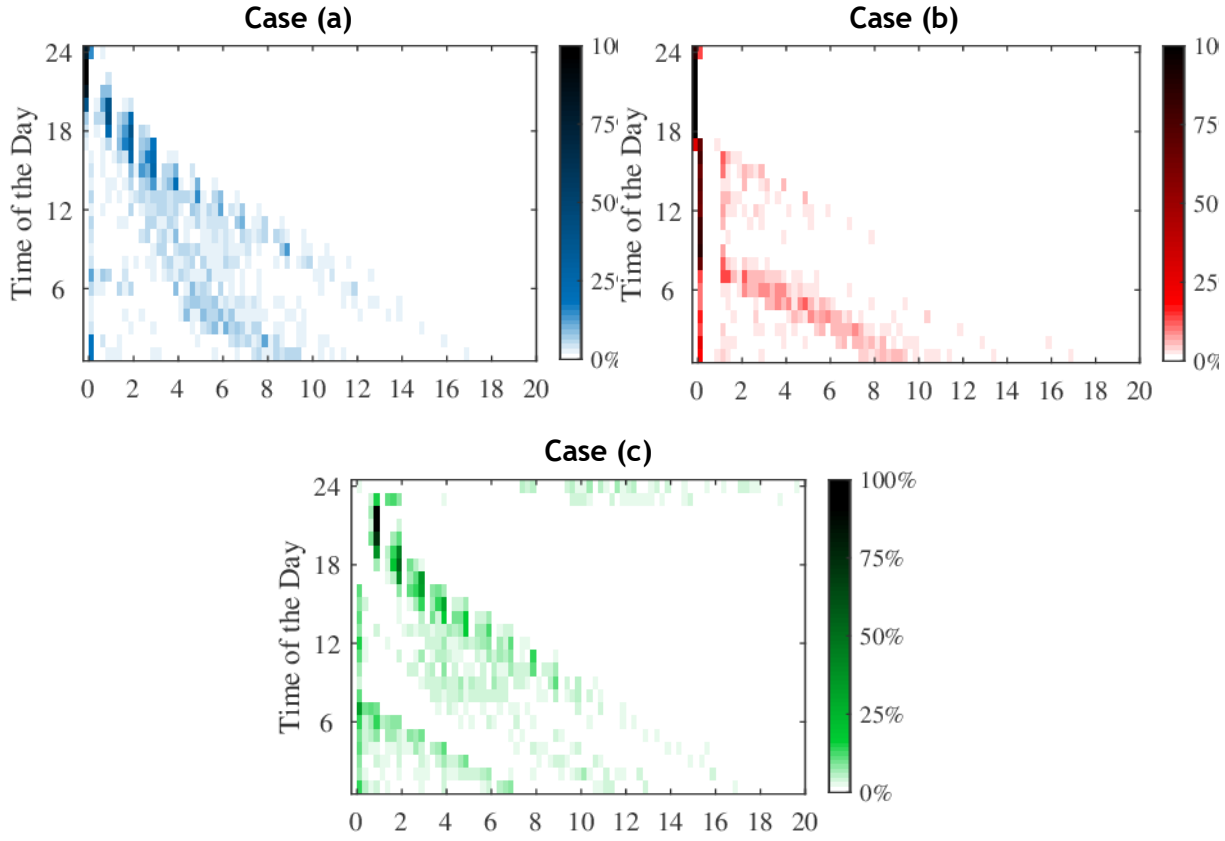

Figure 12: Relative shares of achievable PIT in simulation, based on the objective applied in grid-connected operation and sorted by the starting time of the islanding event.

In case (a) the MG operator could naturally achieve the lowest overall operational cost, although the total amount of energy exchanged with the main grid was noticeably higher than in case (b). Energy storage charges during night and early morning when electricity prices are low, and discharges during peak price hours, which coincides relatively well with peak demand periods.

Case (b) leads to minimum energy exchange with the main grid. The MG achieves a maximum local utilization of its resources. This also constitutes the lowest overall power flows, currents and line losses among the investigated cases. The BESS is not often used, since the losses associated with the utilization conflict with the objective. Demand significantly exceeds generation capacity as the total of import of energy in 100 days of operation was about 50 times higher than the import in the simulation.

In case (c), the DSO's demand for maximum PIT degrades performance of the secondary cost minimization. Main causes are single power purchases in high priced hours to charge electric and thermal storage and provide reserves for a possible disconnection from the main grid.

In a later stage, the EMS was extended to include a more accurate approximation of the cost of battery energy storage system wear, as opposed to the simplified linear and quadratic functions of power, which are employed by the majority of works. Parameter variation has been performed for a weighted, linear combination of four objectives in a 48-h simulation of the generic MG test system [27].

Four performance metrics are introduced to compare the simulation results:

- T_c is the total cost incurred within the 48-h period.
- T_P is the total net energy exchanged with the main grid within the 48-h period.
- T_{PIT} is the average potential islanding time (PIT) achievable at one single time step in the future, as planned by the EMS.
- T_{Loss} is the energy loss incurred within the 48-h period.

The performance metrics are chosen to illustrate the trade-off to be made. Figure 13 provides a heat map of the correlation coefficients between the vectorized performance metrics of all scenarios. They are used to visualize the relationship between the four different objectives.

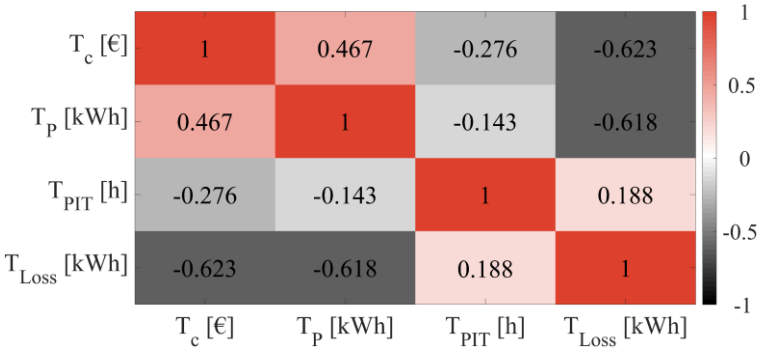

Figure 13: Heat map of correlation coefficients between performance metrics

Both, cumulative cost T_c and energy exchange T_P appear to be negatively correlated with the average PIT. It has been shown that maximizing the PIT leads to a more conservative operation of energy storage to withhold resources to supply load.

If the MG is scheduled to withhold resources for islanding operation even in peak demand hours and to plan for islanding operation, excessive load peaks can be avoided. These results are further underlined in Table 6. It shows mean PIT, mean SOC of the BESS and mean peak power exchange with the main grid, averaged respectively for all scenarios employing a set value of ρ_{PIT}.

Table 6: Evaluation in reference to PIT scaling

	$\rho_{PIT} = 1$	$\rho_{PIT} = 2$	$\rho_{PIT} = 6$	$\rho_{PIT} = 24$
$\overline{T}_{PIT}$ [h]	6.74	7.84	9.27	9.72
$\overline{SOC}_{BESS,6}$	0.77	0.80	0.85	0.86
$\overline{p}_1^{Max}$ [kW]	7.28	7.33	7.32	6.37

Earlier project deliverables defined the key performance indicators (KPI). In the following, a subset of KPI results of the presented control simulation is presented.

The testing of hosting capacity increase depends not merely on the configuration of the MPC objectives, but rather on the simulation period. Heat pumps can be used for DSR only in heating periods. Thus, in summer months, since there is hardly any heat demand, the flexibility potential would be minimal. The presented results are based on simulation (see Table 7 and Table 8), which are fed with Simris consumption data from October 2018. For

the heat demand, generic profiles have been applied. These profiles derive from an integrated thermal-electrical demand model [28], which is based on a bottom-up activity-based structure, using stochastic programming techniques.

Flexibility

The « Flexibility » KPI describes the available energy flexibility that can be allocated at a specific grid segment and thus quantifies, how much of the available storage capacity of a segment is used.

For this purpose, the average SOC of a given asset was measured over a period of 24 hours. The results are presented in Table 7. They show that an especially high flexibility usage is achieved when minimizing the energy exchange or the grid losses. In case of the energy exchange minimization, this is due to the objective's preference for maximum local utilization of resources.

In case of the grid loss optimization, the MPC optimization routine prefers shorter power transmission distances due to lower line resistance, which promotes the utilization of local flexibilities.

Table 7: Relative flexibility utilization

	Baseline (not controlled)	Equally weighted objectives	Minimize Energy Exchange	Maximize PIT	Minimize Cost	Minimize Grid Losses
Li-Ion BESS	30.60%	19.03%	72.01%	19.79%	42.39%	62.88%
Boiler	28.82%	29.01%	44.84%	20.22%	44.95%	45.32%
Heat pump	34.47%	29.94%	34.38%	28.99%	39.90%	51.00%
Redox Flow BESS	50.64%	47.75%	55.45%	46.81%	51.17%	56.93%
Household BESS	49.50%	19.86%	83.31%	23.07%	30.33%	67.40%

Increase in Hosting Capacity

The « Increase in hosting capacity » KPI describes how much additional DER capacity can be achieved by using energy flexibilities and advanced control in comparison to the standard hosting capacity without smart grid solutions (e.g. RBC).

In this analysis the hosting capacity is defined as the maximum internal peak load that occurs within the MG, including the charging power of all assets. Table 8 shows that the hosting capacity increase is lowest in case of the energy exchange minimization. This is due to the algorithm's effort to reduce the internal electrical load at times of low energy production in order to avoid energy imports from the main grid. It is important to note that the KPI itself is not subject to optimization.

Overall, the results indicate that the MPC enables higher hosting capacity in all regarded cases, which suggests that implementing the MPC in the system may permit to integrate more RES into the grid. However, the results must be interpreted with care as the simulation

is based on a single dataset that had been available at the time. Thus, the results only indicate the tendency of the MPC in combination with a particular objective to increase hosting capacity. A Monte-Carlo-based analysis over a longer time horizon is recommended to support the findings.

Table 8: Potential hosting capacity increase due to DSR activation using MPC in 24-h test.

	Baseline (RBC)	Equally weighted objectives	Minimize Energy Exchange	Maximize PIT	Minimize Cost	Minimize Grid Losses
Peak Load in kW (24h)	542	804	594	712	781	708
Hosting Capacity increase	-	49%	10%	32%	44%	31%

4.3.2 Agent-Based Concept

The methodology presented in section 3.1.4 is evaluated for one representative week in autumn 2018. Hence, the simulation time is set to 144 hours, with input and control signals at hourly granularity and a forecast horizon of 24 hours. The optimization as well as the simulation is based on the model presented in section 3.1.1.

Table 9: Multi-agent use case results [20]

Stakeholder	Locally optimal cost	Globally optimal cost	Final cost including payoff	Relative cost reduction
MG 1	-1530.55€	-1530.54€	-15550.07€	1.28%
MG 2	921.40€	926.68€	901.83€	2.12%
MG 3	-186.92€	-145.40€	-206.49€	10.47%
MG 4	-1263.30€	-1180.48€	-1282.87€	1.55%
MG 5	2075.93€	2075.94€	2056.36€	0.94%
MG 6	-934.81€	-934.73€	-954.38€	2.09%
MG 7	-1160.81€	-1100.92€	-1180.38€	1.69%
MG 8	2030.91€	2397.64€	2011.35€	0.96%
DSO	1098.78€	367.36€	1079.21€	1.78%
Entire System	**1050.68€**	**874.55€**	**874.55€**	**16.76%**

Table 9 provides an overview on the results for the described multi-MG scenario. By comparing the locally optimal cost, which are a result of the individual optimization on MG level, with the globally optimal cost, which are a result of the system optimization including the DSO objectives, one can see that the costs per MG slightly increase, whereas the cost for the DSO decrease significantly. This is due to the fact that the locally optimal power schedules violate the maximum line capacity of 5.45 MVA at the HV/MV link as illustrated in Figure 14. As a consequence of the locally optimal schedules, the DSO is subject to additional costs of 415.33€ for exceeding the line capacity. For the globally optimal schedules however, no violations occur as the global optimization takes DN constraints by design into account. Consequentially, this leads to a total cost reduction from initially 1050.68€ to 874.55€ for the entire multi-MG system, which corresponds to relative cost savings of up to 16.76%.

In order to realize the cost reduction, the MGs must, however, deviate from their original cost-optimal schedule leading to - from their perspective - suboptimal cost. The NBS method is applied to financially reimburse the MGs for their participation in the overall reduction of system cost. In Table 9 one can notice that the total cost of the system remain 874.55€ as bilateral payments are being made between the agents. As a result, every agent realizes a cost reduction in comparison to their original locally optimal cost. Although the individual cost reduction is rather low for most of the MGs and the DSO, the results indicate that it is still worth to apply the NBS strategy due to the previously mentioned win-win situation. For an elaboration on this topic, especially with regard to the use case setup, please refer to the corresponding publication [20].

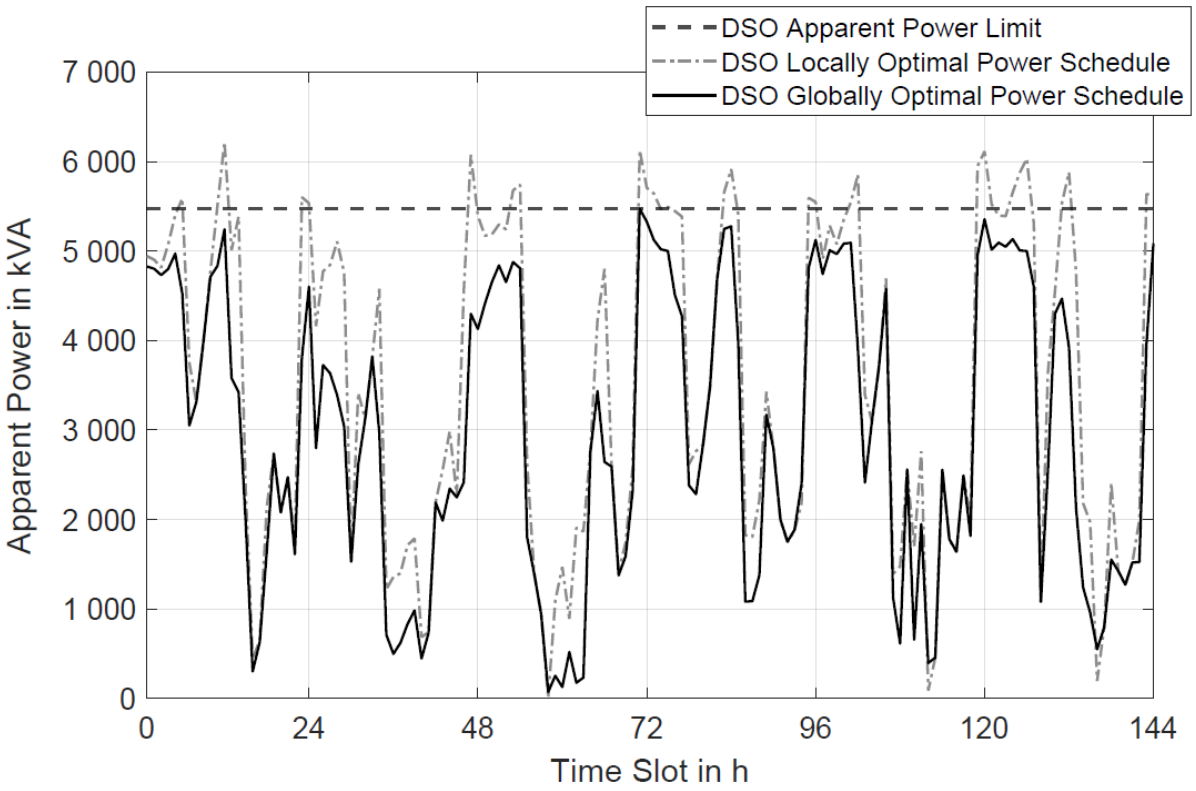

Figure 14: DSO's locally and globally optimal power schedules [20]

4.4 Summary

In the first section of this chapter, two different forecasting strategies have been evaluated. It has been shown that, given sufficient high-quality data, they perform at state-of-the-art level.

The second part of this chapter presents briefly the main results of the control method evaluation. It is shown that the MPC clearly outperforms the RBC. The evaluation of different KPIs suggest that the MPC is well-suited for MG asset control. Finally, the agent-based concept has been evaluated using a multi-MG use case based on the Simris demonstrator.

For more details on the described methodology and the presented results, please refer to the corresponding publications as indicated in the respective sections.

5 RESULTS OF IMPLEMENTING INTELLINGENCE MODULE

5.1 Forecasts

The results of the forecasting module are shown in Figure 155. The figure is divided into four rows. Namely predictions of demand, PV production, wind turbine generation and the difference between generation and demand. The straight line shows the time of observation. On the left side of the straight line, there is the historical data. The small circles around the line represent actual observations. On the right side there is one coloured line, which represents forecast for the next 24 hours.
The grey lines show possible variations in the forecasts. The column diagrams on the right side demonstrate the differences between the prediction and the observation in kW. Values of zero or nearby indicate very accurate forecasts. As more they move apart the less accuracy is given. While the errors of the demand and PV production forecasts are following the normal distribution, the forecasts of wind turbine generation tend to be lower than observed. Thus, the residual load, a sum of the three forecasts mentioned above, tends to be lower than observed, too.

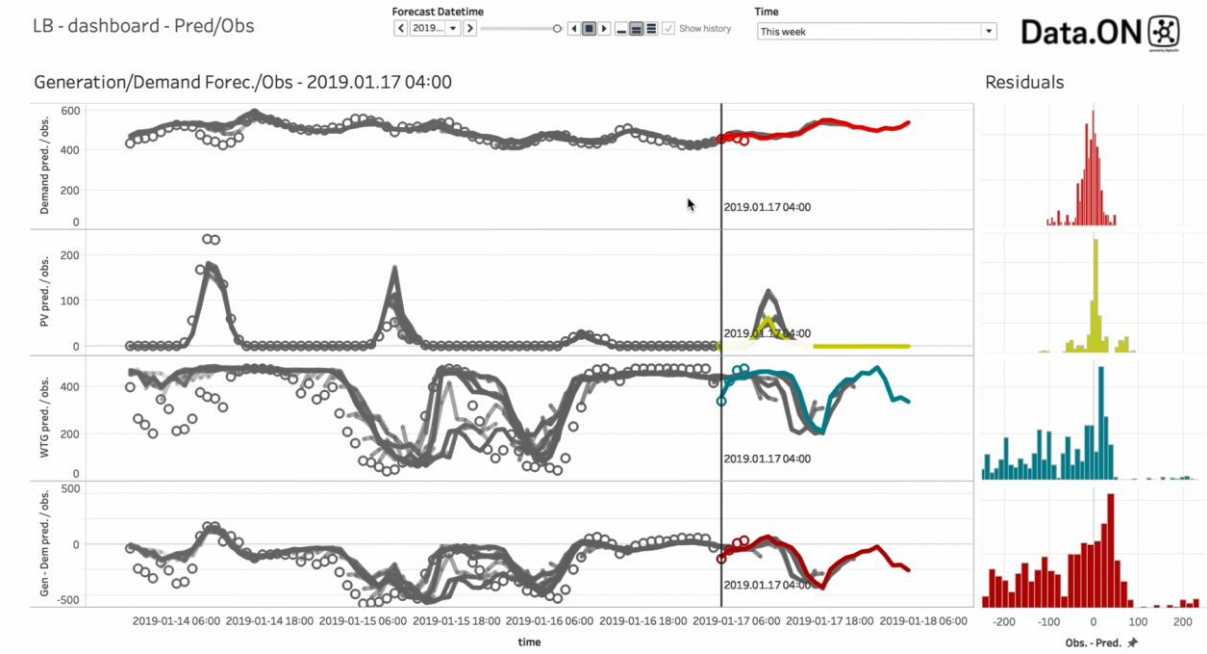

Figure 15: Forecast accuracy

5.2 Control methods

Figure 166 presents the behaviour of the battery as result of the optimization process. Three rows are indicating the setpoint prediction, the battery SOC prediction and the day-ahead energy price. The left side of the straight line are the already past values. On the right side there are the coloured optimized pathways, which are to be followed and the prediction of the day ahead energy price. Both the forecast and optimization data utilize a 24hr rolling window for data collection.

The result of how the optimization works will be explained in the first two battery cycles. At the starting point (1) the setpoint for the grid connection is at zero and the battery is empty. The day ahead price is comparatively low (2). The battery is charged. The dynamic energy price has risen and battery energy sold to the grid (3). After the full discharge of the battery the energy price is still high but the battery charges anyway using energy from overproduction then (4). The optimization includes the forecasting and so it predicts the future energy price increase (5). At this point the battery discharge again and is effectively shaving the peak.

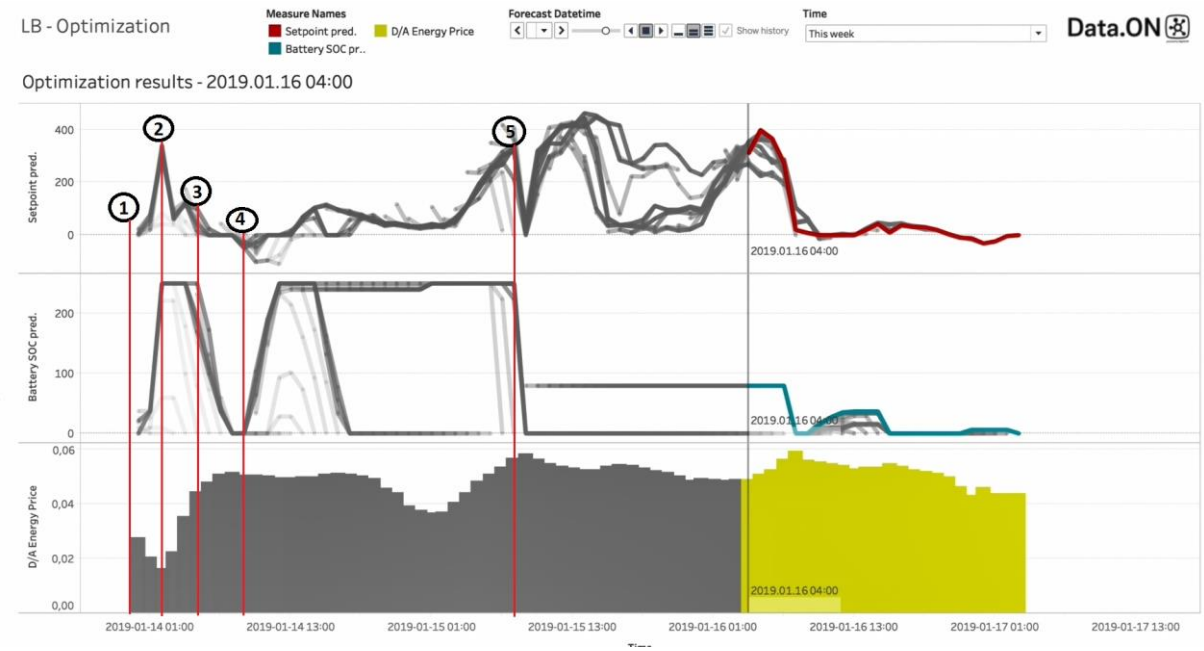

Figure 16: Set point and battery SOC behaviour

6 TECHNO-ECONOMIC MODEL

Table 1010 shows the results of the comparison between the operational costs within different setups described in Section 3.3. Savings above ten percent can be reached by adding the forecasting and optimization modules and are primarily achieved by reducing peak loads. While a big impact can be seen comparing rule-based control to the other settings, it is only a small improvement regarding savings from case 2 to case 3. The results indicate that a forecasting period of 24 hours is sufficient to provide similar cost savings compared to perfect foresight for the whole period.

Table 10: Results of the techno-economic model

Case	Technical Setting	Foresight Level	Operational Costs	Savings
1	Rule-based control	No foresight	65.615 €	0 %
2	EMS with optimization and forecasting module	Perfect foresight for the whole period	56.286 €	14 %
3	EMS with optimization and forecasting module	Perfect foresight for one day	57.101 €	13 %

The design of the tariff structure in Sweden penalises peaks and by having the minimisation of cost as the main objective of the optimization module, peak-shaving is achieved as an “indirect” benefit, hence providing value for both the customer and the DSO (the main grid in south of Sweden is constrained in the demand direction). In this way, the project was able to create benefit for both the customer and the DSO as cost was minimised for the customer and the DSO benefits from peak-shaving behaviour from the micro grid as an ancillary service. The magnitude of the cost saving and the subsequent peak-shaving is a function of energy storage capacity and the Simris micro was not designed to be optimally sized to deliver maximum value but as a proof of concept.

7 SUMMARY

In order to create techno-economic models to assess the impact of forecasting and optimization algorithms in the local energy system implemented in Simris, diverse requirements have to be fulfilled. To facilitate theoretical investigation of the system, an accurate grid model was developed. Theoretical simulations and development of advanced power analytics have been conducted by RWTH Aachen university, while E.ON Energidistribution AB has developed forecasting and optimized control adapted to the conditions prevailing in Simris.

Regarding the forecasting methods, RWTH Aachen investigated various forecasting techniques focusing on different objectives. The most accurate forecast of the PV production and the load behavior is reached by using a sequence-to-sequence algorithm based on recurrent neural networks. As WT generation is more stochastic, the forecasting results could be improved by using a convolutional recurrent neural network to exploit spatial as well as temporal dependencies in the data.

On E.ONs side there were two different approaches. Using data from different weather data providers and the load data collected in Simris, E.ON applied one ML algorithm on every single forecast quantity in the first approach. The second approach was to apply one ML algorithm for the combined data of the different forecasting values.

RWTH Aachen developed an MPC approach that works in a receding horizon fashion. At each time-step, the control input is optimized based on the simulation of the grid model according to a specified objective function. This way it can take forecasts into account. Furthermore, the developed MPC allows multiple objectives such as loss minimization or potential islanding time maximization.

The optimization module created by E.ON calculates the optimal steering strategy for the LES based on predicted energy generation and consumption over the next 24 hours. Depending on the specific customer segment and market condition, different optimization objectives can be set, which will be defined according to customer needs.

Finally, RWTH Aachen developed an agent-based concept, which was derived in a multi-microgrid scenario where each MG as well as the DSO were regarded as agents. The method uses Nash bargaining solution to find an allocation of resources – in our case the usage of the distribution network - that balances the agents' conflicting objectives. The concept can be easily adapted to other scenarios.

Besides technical aspects, E.ON assessed the use case from a techno-economic perspective as well. The comparison between a heuristic rule-based control system and an optimization-based control system that can incorporate forecasts and shows that adding the intelligence module leads to savings of operational costs above ten percent in the considered case.

8 RECOMMENDATIONS AND FUTURE STEPS

8.1 Recommendations

For developing forecasting approaches, the quality and amount of data is highly relevant. Improving results in choosing the best-suited solution for forecasting can be achieved. Considering the forecast of wind generation, there is an advantage of taking a higher quantity of measuring points allocated in the surrounding on the one hand. On the other hand, it would be valuable, if the velocity of wind is measured in different heights.
However, the usage of model predictive control or optimization methods in conjunction with forecasting is from a technical as well as an economic perspective beneficial. The optimization provides an increasing performance compared to a heuristic, rule-based control.

8.2 Future steps

A real MPC based on the simulations can be implemented on the project site. To prove and test the agent-based control several MGs can be defined and interconnected. Worth investigating is also the attempt on how to scale the solution and test the behavior on different settings of parameters and objectives.

9 REFERENCES

[1] J. Machowski, J. Bialek and D. J. Bumby, Power System Dynamics: Stability and Control, Wiley, 2008.

[2] J. Schiffer, D. Zonetti, R. Ortega, A. M. Stanković, T. Sezi and J. Raisch, "A survey on modeling of microgrids—From fundamental physics to phasors and voltage sources," *Automatica,* vol. 74, pp. 135-150, 12 2016.

[3] A. Bidram and A. Davoudi, "Hierarchical Structure of Microgrids Control System," *IEEE Transactions on Smart Grid,* vol. 3, pp. 1963-1976, 12 2012.

[4] J. M. Guerrero, J. C. Vasquez, J. Matas, L. G. Vicuna and M. Castilla, "Hierarchical Control of Droop-Controlled AC and DC Microgrids—A General Approach Toward Standardization," *IEEE Transactions on Industrial Electronics,* vol. 58, pp. 158-172, 1 2011.

[5] O. Palizban, K. Kauhaniemi and J. M. Guerrero, "Microgrids in active network management—Part I: Hierarchical control, energy storage, virtual power plants, and market participation," *Renewable and Sustainable Energy Reviews,* vol. 36, pp. 428-439, 8 2014.

[6] D. Mildt, M. Cupelli, A. Monti and R. Kubo, "Islanding Time Evaluation in Residential Microgrids," in *IEEE PES/IAS PowerAfrica*, 2018.

[7] M. Bogdanovic, H. Wilms, M. Cupelli, M. Hirst, L. A. H. Salmeron and A. Monti, "Technical Management of a Grid-Connected Microgrid that can run in an Islanded Mode with 100% Renewable Generation," *CIRED Workshop "Microgrids and local energy communities",* 6 2018.

[8] H. Wilms, D. Mildt, M. Cupelli, A. Monti, P. Kjellen, T. Fischer, D. Panic, M. Hirst, E. Scionti, S. Schwarz, P. Kessler and L. Hernandez, "Microgrid Field Trials in Sweden: Expanding the Electric Infrastructure in the Village of Simris," *IEEE Electrification Magazine,* vol. 6, pp. 48-62, 12 2018.

[9] S. Hochreiter and J. Schmidhuber, "Long short-term memory," *Neural computation,* vol. 9, no. 8, pp. 1735-1780, 1997.

[10] L. J. Ba, R. Kiros and G. E. Hinton, "Layer Normalization," *CoRR,* vol. abs/1607.06450, 2016.

[11] H. Wilms, M. Cupelli and A. Monti, "Combining auto-regression with exogenous variables in sequence-to-sequence recurrent neural networks for short-term load forecasting.," in *IEEE 16th International Conference*, 2018.

[12] P. J. Werbos, "Backpropagation through time: what it does and how to do it," *Proceedings of the IEEE,* vol. 78, pp. 1550-1560, 1990.

[13] J. Bergstra and Y. Bengio, "Random Search for Hyper-Parameter Optimization," *Journal of Machine Learning Research,* vol. 13, pp. 281-305, 2012.

[14] N. Srivastava, G. Hinton, A. Krizhevsky, I. Sutskever and R. Salakhutdinov, "Dropout: A Simple Way to Prevent Neural Networks from Overfitting," *J. Mach. Learn. Res.*, vol. 15, pp. 1929-1958, 1 2014.

[15] K. Hara, D. Saitoh and H. Shouno, "Analysis of Dropout Learning Regarded as Ensemble Learning," in *Artificial Neural Networks and Machine Learning – ICANN 2016*, Springer International Publishing, 2016, pp. 72-79.

[16] H. Wilms, M. Cupelli, A. Monti and T. Gross, "Exploiting Spatio-Temporal Dependencies for RNN-based Wind Power Forecasts," in *IEEE GTD Asia 2019*, 2019.

[17] X. Shi, Z. Chen, H. Wang, D.-Y. Yeung, W.-K. Wong and W.-c. Woo, "Convolutional LSTM Network: A Machine Learning Approach for Precipitation Nowcasting," *CoRR,* vol. abs/1506.04214, 2015.

[18] G. Gürses-Tran, D. Mildt, M. Hirst, M. Cupelli and A. Monti, "MPC based Energy Management Optimization for a European Microgrid Implementation," in *25th International Conference on Electricity Distribution, CIRED, forthcoming*, 2019.

[19] J. F. Nash, "The Bargaining Problem," *Econometrica,* vol. 18, no. 2, p. 155, 1950.

[20] G. Gürses-Tran, S. Schwarz, H. Flamme, M. Cupelli and A. Monti, "Agent-based Power Scheduling Framework for Interconnected Local Energy Communities Incorporating DSO Objectives," *submitted to IECON 2019 - 45th Annual Conference of the IEEE Industrial Electronics Society, Lissabon, Portugal,* 2019.

[21] T. Hong, P. Pinson, S. Fan, H. Zareipour, A. Troccoli and R. J. Hyndman, "Probabilistic energy forecasting: Global Energy Forecasting Competition 2014 and beyond," *International Journal of Forecasting,* vol. 32, pp. 896-913, 7 2016.

[22] W. Kong, Z. Y. Dong, Y. Jia, D. J. Hill, Y. Xu and Y. Zhang, "Short-Term Residential Load Forecasting Based on LSTM Recurrent Neural Network," *IEEE Transactions on Smart Grid,* vol. 10, pp. 841-851, 1 2019.

[23] A. Géron, Hands-On Machine Learning with Scikit-Learn and TensorFlow, O'Reilly UK Ltd., 2017.

[24] S. Seabold and J. Perktold, "Statsmodels: Econometric and statistical modeling with python," in *9th Python in Science Conference*, 2010.

[25] K. Strunz, E. Abbasi, R. Fletcher, N. Hatziargyriou, R. Iravani and G. Joos, TF C6.04.02 : TB 575 -- Benchmark Systems for Network Integration of Renewable and Distributed Energy Resources, 2014.

[26] S. Papathanassiou, N. Hatziargyriou and K. Strunz, "A Benchmark Low Voltage Microgrid Network," *CIGRE Symposium,* 1 2005.

[27] M. C. A. M. D. Mildt, "Objective Trade-off in MPC Based Enery Management for Microgrids," *IEEE PES GTD Proceedings,* 2019.

[28] E. McKenna, M. Thomson and J. Barton, "CREST Demand Model," 2 2019.

[29] H. Wilms, M. Cupelli and A. Monti, "On the Necessity of Exogenous Variables for Load, PV and Wind Day-Ahead Forecasts using Recurrent Neural Networks," in *IEEE Electrical Power and Energy Conference (EPEC)*, 2018.

[30] S. H. Low, "Convex Relaxation of Optimal Power Flow—Part I: Formulations and Equivalence," *IEEE Transactions on Control of Network Systems,* vol. 1, pp. 15-27, 3 2014.

[31] T. O. Kvalseth, "Cautionary Note about R 2," *The American Statistician,* vol. 39, p. 279, 11 1985.

[32] I. Sutskever, O. Vinyals and Q. V. Le, "Sequence to Sequence Learning with Neural Networks," *CoRR,* vol. abs/1409.3215, 2014.

[33] J. Lofberg, "YALMIP : a toolbox for modeling and optimization in MATLAB," in *2004 IEEE International Conference on Robotics and Automation (IEEE)*, 2004.

[34] R. Pascanu, T. Mikolov and Y. Bengio, "On the difficulty of training recurrent neural networks.," in *ICML (3)*, 2013.

10 APPENDICES

10.1 Appendix 1 – Figures of forecasting methods

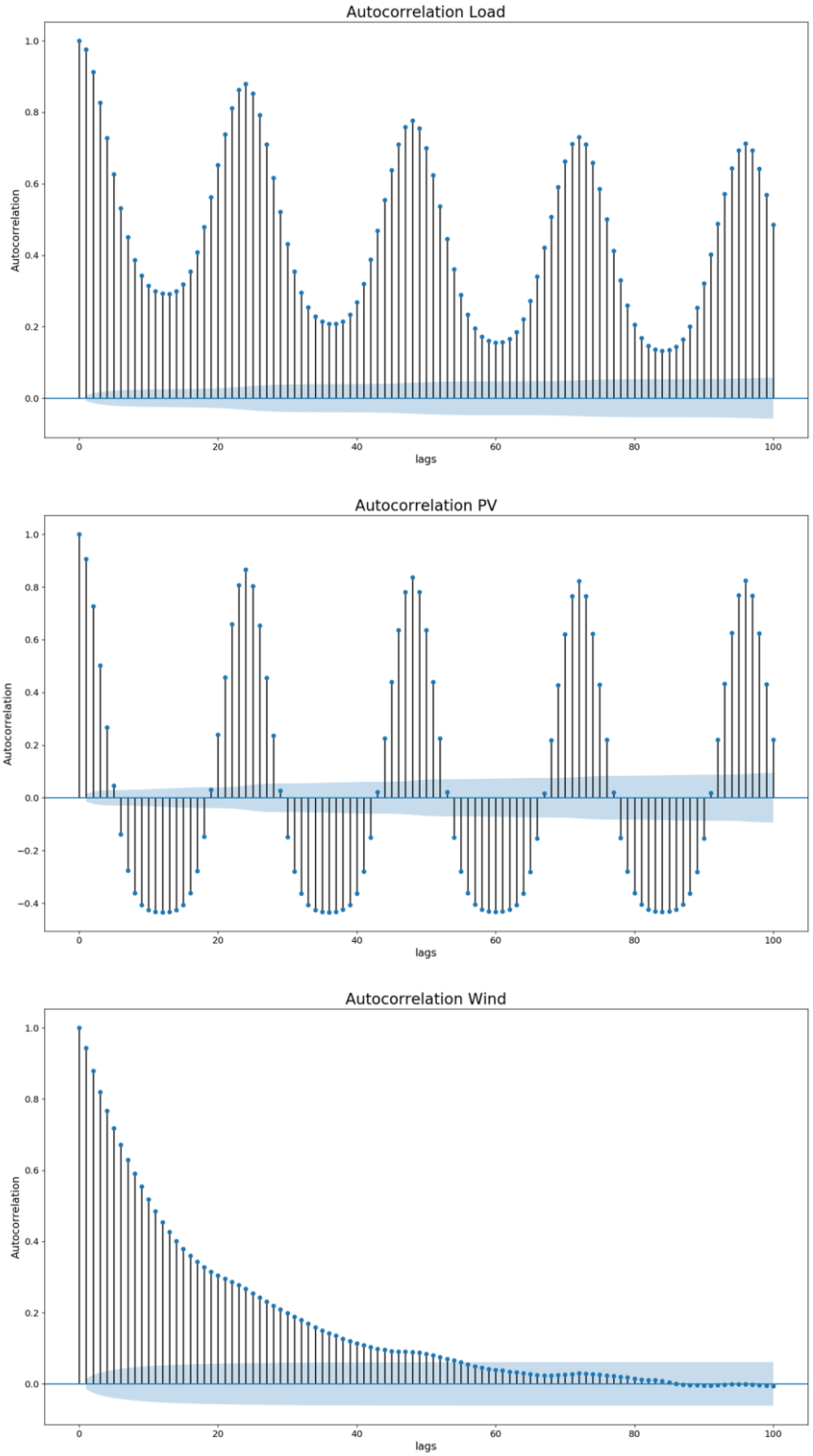

Figure 17: Autocorrelation of load, PV and wind time-series [29]

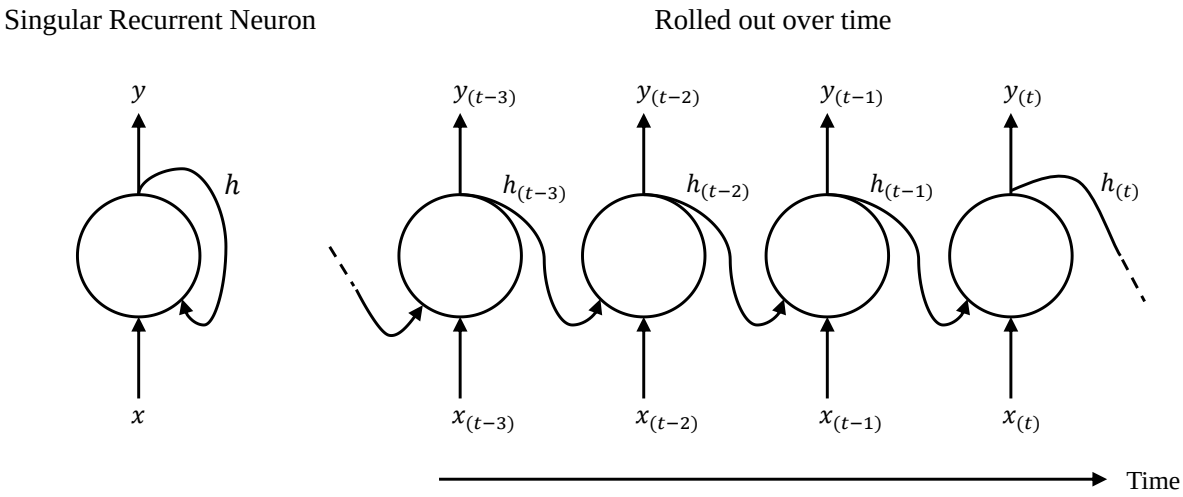

Figure 18: Recurrent neuron rolled out over time [11]

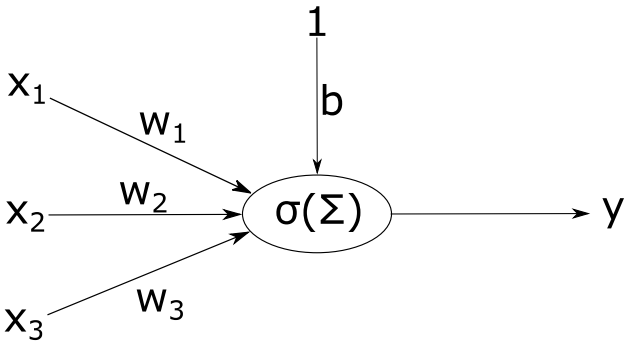

Figure 19: Illustration of a neuron. The input vector x is weighted using the parameter vector w. The sum over all weighted inputs is taken and a bias b is added. The result is modified using the activation function σ.

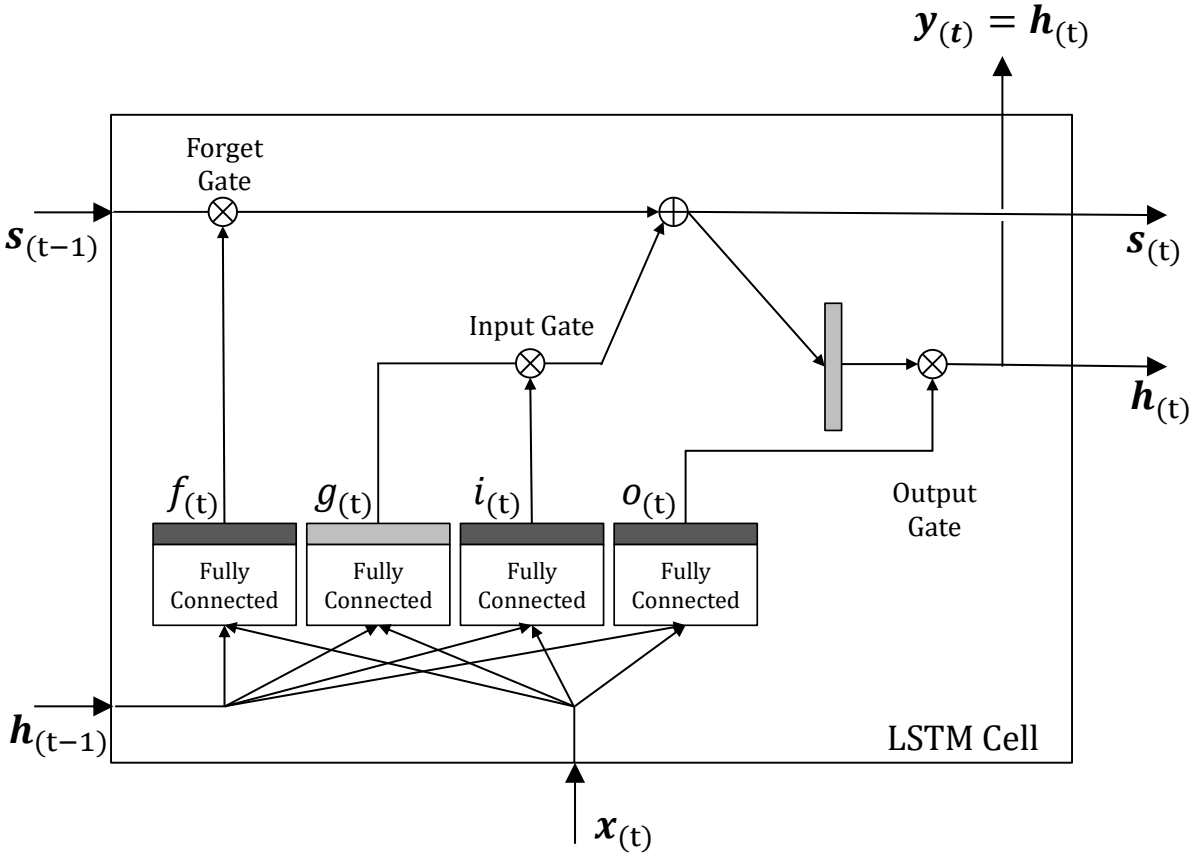

Figure 20: LSTM cell [11]

10.2 Appendix 2 - Description and assumptions of the electrical grid model

Loads

The consumers are treated as PQ loads, which ensures that - as a result of a load flow calculation - the bus voltage and angle are determined according to the specified real power *P* and reactive power *Q*. As an input, at each time step the active power time series are loaded into the model. The reactive power is computed based on the specified power factor. The power time series are treated as being deterministic and known. However, they can be changed after each time step in order to accommodate forecasting procedures.

BESS

The battery energy storage systems (BESS) are modeled statically. At each time step, a BESS has a certain energy level that corresponds to the state of charge (SOC). The energy level is controlled by the charging and discharging power. Each BESS is characterized by its charging and discharging efficiency, its maximum charging and discharging power as well as lower and upper bounds on the batteries' SOC. BESS are typically connected to the grid via DC-AC inverters. The controllable reactive power output is limited by the maximum apparent power of the inverter, which is usually slightly over-dimensioned with regard to the maximum

power output of the connected component (in this case the BESS), thus increasing the reactive power capabilities of the system.

Heat Pumps and Hot Water Boilers

Heat pumps and hot tap water boilers are treated as partially deferrable loads that ensure that the thermal room temperature and water temperature demand is met at any time. The model couples this thermal demand with the electric power that is required to operate it. Flexibility is created by the thermal energy storage. The model can consider thermal losses as well as minimum and maximum capacity limits and electric power limits. In the target system under study, however, the thermal losses are negligible and thus have been neglected. Analogously to the deterministic PQ loads, the reactive power demand is determined using the heat pumps' power factor.

Micro Turbines

The active power generation of a micro turbine such as a diesel generator has a minimum power output when in operation and can produce up to the generator's nominal power. Furthermore, the model assumes that the generator permits full two quadrant control such that the generator can both produce inductive and capacitive reactive power. Reactive and active power are both limited by the maximum apparent power. Additionally, the ramp rate of the micro turbine is limited.

Additional Microgrid Assets

The grid model also permits adding electric vehicle charging stations if required. The modeling is done very similar to the BESS model, with the difference that their connection time is limited. For the sake of simplicity, it is assumed that the connection patterns are known a-priori, which means that the EV's SOC when it connects to the charging station is predefined and fixed. Furthermore, in order to fulfill the user demand, the final SOC before disconnection must not be below a certain energy level.

The distributed generation units can be classified into controllable and volatile energy resources.

Analogously to BESS, the inverter provides reactive power control capabilities.

Photovoltaics are characterized by the same characteristics. In contrast to fuel cells, their active power generation is defined by the current weather conditions. Therefore, analogously to the PQ loads, the power output is defined using external time series.

Wind generation units are - similarly to PVs - volatile. As such, their active power is also predefined.

Assumptions for the Load Flow Simulation

The power lines of the microgrid are modeled using their complex line impedances. Admittance and susceptance are neglected. Since the distribution grid follows a tree structure, the DistFlow formulation of the power flow equations is used in combination with the relaxation to a second order cone problem, as explained in [30]. The main grid serves as a slack bus, which allows to balance the active and reactive power in the simulated system. The power flow through the transformer, however, is limited by the nominal transformer power.

Islanding operation is effectively controlled using an additional binary variable that represents the circuit breaker, which separates the microgrid from the overlying distribution grid; thus, the energy flow between the networks is discontinued. During islanding, a

sufficiently-sized battery is assumed at the disconnected bus as the new, grid forming element.

10.3 Appendix 3 – Simplified DN to illustrate the agent-based concept

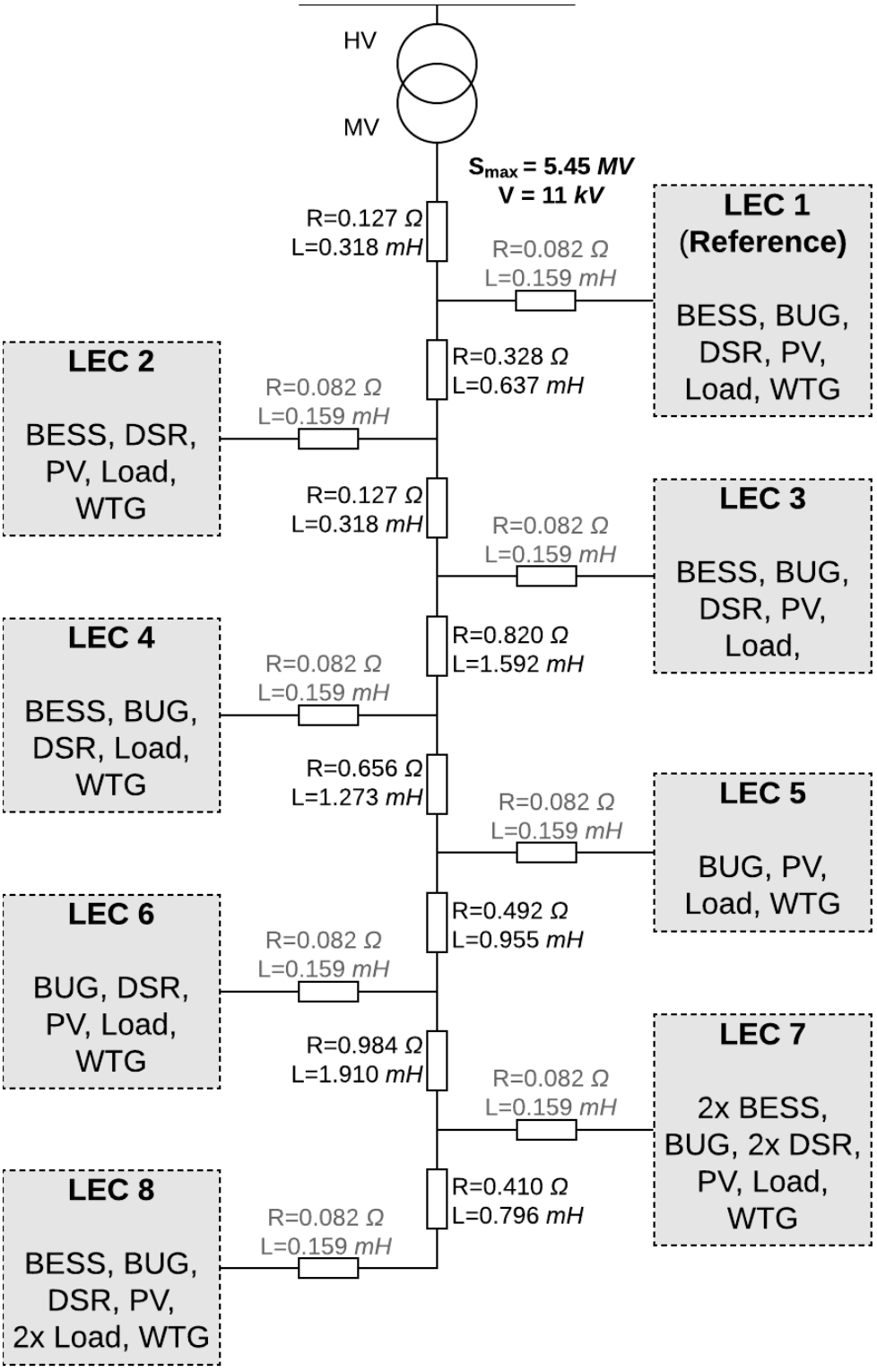

Figure 21: Distribution network illustrating the composition of the MGs.

10.4 Appendix 4 – Nash bargaining formular

$$\max_{\{p_{DSO,MG_i}\}} \underbrace{\left(c'_{DSO} - c''_{DSO} - \sum_{\forall i} p_{DSO,MG_i}\right)}_{\text{Payoff for DSO}} \cdot \prod_{\forall i} \left(\underbrace{c'_{MG_i} - c''_{MG_i} + p_{DSO,MG_i}}_{\text{payoff for MG i}}\right) \quad (1)$$

$$\max_{\{p_{DSO,MG_i}\}} \underbrace{\left(c'_{DSO} - c''_{DSO} - \sum_{\forall i} p_{DSO,MG_i}\right)}_{\text{Payoff for DSO}} \cdot \prod_{\forall i} \left(\underbrace{c'_{MG_i} - c''_{MG_i} + p_{DSO,MG_i}}_{\text{payoff for MG i}}\right)$$

$$\text{s.t.} \quad 0 \leq \left(c'_{MG_i} - c''_{MG_i} + p_{DSO,MG_i}\right) \quad \forall i$$

$$0 \leq c'_{DSO} - c''_{DSO} - \sum_{\forall i} p_{DSO,MG_i}$$

10.5 Appendix 5 – Metrics for forecast evaluation

Three metrics were chosen to evaluate the developed model: The *R^2 accuracy measure*, the *root mean square error* (RMSE) and the *normalized RMSE* ($nRMSE_{\%}$). The R^2 accuracy measure is defined as

$$R^2 = 1 - \frac{\sum_{i=1}^{N}(y_i - \hat{y}_i)^2}{\sum_{i=1}^{N}(y_i - \bar{y})^2} \quad (2)$$

with i denoting each prediction $\hat{y}_i$ and each target value y_i for all N sequences in the validation data set, and $\bar{y}$ being the sample mean of the targets [31]. The metric describes the explained variance by the model and its inputs in relation to the total variance. Values close to one are typically preferable. The RMSE is the most common metric to assess the accuracy in a regression problem. A low value corresponds to a low standard deviation of the residuals. It is defined as

$$RMSE = \sqrt{\frac{1}{N}\sum_{i=1}^{N}(y_i - \hat{y}_i)^2} \quad (3)$$

For better interpretation, the $nRMSE_{\%}$ is calculated by dividing the RMSE by the range of the target values:

$$nRMSE_{\%} = \frac{RMSE}{y_{max} - y_{min}} \times 100 \quad (4)$$